
Increasing the Scope as You Learn: Adaptive Bayesian Optimization in Nested Subspaces

Leonard Papenmeier
Lund University
leonard.papenmeier@cs.lth.se

Luigi Nardi
Lund University, Stanford University, DBTune
luigi.nardi@cs.lth.se

Matthias Poloczek*
Amazon
San Francisco, CA 94105, USA
matpol@amazon.com

Abstract

Recent advances have extended the scope of Bayesian optimization (BO) to expensive-to-evaluate black-box functions with dozens of dimensions, aspiring to unlock impactful applications, for example, in the life sciences, neural architecture search, and robotics. However, a closer examination reveals that the state-of-the-art methods for high-dimensional Bayesian optimization (HDBO) suffer from degrading performance as the number of dimensions increases or even risk failure if certain unverifiable assumptions are not met. This paper proposes BAXUS that leverages a novel family of nested random subspaces to adapt the space it optimizes over to the problem. This ensures high performance while removing the risk of failure, which we assert via theoretical guarantees. A comprehensive evaluation demonstrates that BAXUS achieves better results than the state-of-the-art methods for a broad set of applications.

1 Introduction

The optimization of expensive-to-evaluate black-box functions where no derivative information is available has found many applications, for example, in chemical engineering [11, 28, 31, 58, 60], materials science [23, 29, 30, 32, 52, 64, 68], aerospace engineering [39, 43], hyperparameter optimization [5, 33, 38, 61], neural architecture search [36, 57], vehicle design [14, 34], hardware design [19, 49], drug discovery [51], robotics [12, 13, 41, 46, 54], and the life sciences [18, 59, 65]. Here increasing the number of dimensions (or parameters) of the optimization problem usually allows for better solutions. For example, by exposing more process parameters of a chemical reaction, we obtain a more granular control of the process; for a design task, we may optimize a larger number of design decisions jointly; in robotics, we gain access to more sophisticated control policies.

A series of breakthroughs have recently pushed the envelope of high-dimensional Bayesian optimization and facilitated a wider adoption in science and engineering. The key challenge for further scaling is the so-called curse of dimensionality. The complexity of the task of finding an optimum grows exponentially with the number of dimensions [7, 22]. Recently, methods that rely on local ‘trust regions’ have gained popularity. They usually achieve good performance for problems with up to a couple of dozen input parameters. However, we observe that their performance degrades for higher-dimensional problems. This is not surprising, given that trust regions have a smaller volume but still the full dimensionality of the problem. Other state-of-the-art methods suppose the existence

*The work was done before Matthias joined Amazon.

of a low-dimensional active subspace and enjoy great scalability if they find such a space. The caveat is that its existence is usually not known for practical applications. Moreover, the user needs to ‘guess’ a good upper bound on its dimensionality to enjoy a good sample efficiency.

In this work, we propose a theoretically-founded approach for high-dimensional Bayesian optimization, BAXUS (**B**ayesian optimization with **a**daptively **e**xpanding **s**ubspaces), that reliably achieves a high performance on a comprehensive set of applications. BAXUS utilizes a family of nested embedded spaces to increase the dimensionality of the domain that it optimizes over as it collects more data. As a byproduct, BAXUS can leverage an active subspace, if it exists, without requiring the user to ‘guess’ its dimensionality. BAXUS is based on a novel random linear subspace embedding that enables a more efficient optimization and has strong theoretical guarantees. We make the following contributions:

1. We develop BAXUS that reliably achieves excellent solutions on a broad set of high-dimensional tasks, outperforming the state-of-the-art.
2. We present a novel family of nested random embeddings that has the following properties: a) The BAXUS embedding provides a larger worst-case guarantee for containing a global optimum than the HESBO embedding proposed by [50]. b) The BAXUS embedding is an optimal *sparse embedding*, as defined in Def. 1. c) Its probability of containing an optimum converges to the one of the HESBO embedding as the input dimensionality $D \rightarrow \infty$.
3. We conduct a comprehensive evaluation on a representative collection of benchmarks that demonstrates that BAXUS outperforms the state-of-the-art methods.

The remainder of this paper is structured as follows. Section 2 states the problem and discusses related work. Section 3 presents the BAXUS algorithm and the corresponding embedding. Section 4 evaluates BAXUS on a variety of benchmarks. We give concluding remarks in Section 5.

2 Background

The task is to find a minimizer

$$\mathbf{x}^* \in \arg \min_{\mathbf{x} \in \mathcal{X}} f(\mathbf{x}),$$

where $\mathcal{X} = [-1, +1]^D$. The objective function $f : \mathcal{X} \rightarrow \mathbb{R}$ is an expensive-to-evaluate black-box function. Hence the number of function evaluations needed to find an optimizer is crucial. Evaluations may be subject to observational noise, i.e., $f(\mathbf{x}_i) + \varepsilon_i$, with $\varepsilon_i \sim \mathcal{N}(0, \sigma^2)$. This work focuses on *scalable high-dimensional Bayesian optimization*, where the *input dimensionality* D is in the hundreds, and the sampling budget may comprise a thousand or more function evaluations.

Linear embeddings. A successful approach for HDBO is to assume the existence of an *active subspace* [17], i.e., there exist a space $\mathcal{Z} \subseteq \mathbb{R}^{d_e}$, with $d_e \leq D$ and a function $g : \mathcal{Z} \rightarrow \mathbb{R}$, such that for all \mathbf{x} : $g(T\mathbf{x}) = f(\mathbf{x})$ where $T \in \mathbb{R}^{d_e \times D}$ is a projection matrix projecting \mathbf{x} onto \mathcal{Z} and d_e is the *effective dimensionality* of the problem. In practice, both d_e and \mathcal{Z} are unknown.

REMBO (Random embedding BO) [71] and HESBO (Hashing-enhanced subspace BO) [50] try to capture this active subspace by a randomly chosen linear subspace. Therefore, they generate a random projection matrix S^\top that maps from a d -dimensional subspace $\mathcal{Y} \in \mathbb{R}^d$ with $d \ll D$ (the *target space*) to \mathcal{X} . We call d the *target dimensionality*. For REMBO, each entry in S^\top is normally distributed. REMBO uses a heuristic to determine a hyperrectangle in \mathcal{Y} that it optimizes over. Note that the bounded domain may not contain a point that maps to an optimizer of f , a risk aggravated by distortions introduced by the projection. [6, 8, 9] proposed ideas to mitigate the issue. HESBO’s random projection assigns one target dimension and sign (± 1) to each input dimension. This embedding is inspired by the count-sketch algorithm [15] for estimating frequent items in data streams. The sparse projection matrix S^\top is binary except for the signs, and each row has exactly one non-zero entry. Even though this embedding avoids REMBO’s distortions, as the authors proved, it has a lower probability of containing the optimum [40]. ALEBO [40] uses a Mahalanobis kernel and imposes linear constraints on the acquisition function to avoid projecting outside of \mathcal{X} .

Non-linear embeddings. Several works use autoencoders to learn non-linear spaces for optimization, trading in sample efficiency. Tripp et al. [67] change the training objective of a variational

autoencoder (VAE) [37] to make the target space more suitable for optimization. They give higher weight to better-performing points when training the variational autoencoder (VAE) and show that this improves optimization. Moriconi et al. [47] incorporate the training of an autoencoder directly into the likelihood maximization of a Gaussian process (GP) surrogate. The computational cost is cubic in the number of samples and the input dimension. Lu et al. [42] and Maus et al. [45] use autoencoders to learn embeddings of highly structured input spaces such as kernels or molecules. Other approaches include partial least squares [10] or sliced inverse regression [16].

High-dimensional BO in the input space. A popular approach to make HDBO in the input space feasible is trust regions (TRs) [22, 53, 55, 75]. The TURBO algorithm [22] optimizes over bounded TRs instead of the global space, adapting their side lengths and the center points during the optimization process. By restricting function evaluations to trust regions, TURBO addressed the problem of over-exploration; see [22] for details. Note that the TRs have full input dimensionality, which may impact TURBO’s ability to scale to very large dimensions. Nonetheless, TURBO set a new state-of-the-art by scaling to dozens on input dimensions and thousands of function evaluations. Wan et al. [69] extended the idea of TRs to categorical and mixed spaces by using the Hamming distance to define the TR boundaries. SAASBO [20] uses sparse priors on the GP length scales which seems particularly valuable if the active subspace is axis-aligned. Indeed, SAASBO can outperform TURBO on certain benchmarks [20]. The cost of inference scales cubically with the number of function evaluations; thus, SAASBO is not expected to scale beyond small sampling budgets, which is confirmed by our experiments. Another line of research relies on the assumption that the input space has an additive structure [24, 35, 48, 72]. Additive GPs rely on computationally expensive sampling methods to learn a decomposition of the input variables, which limits the scalability of such methods to problems of moderate dimensionalities and sampling budgets [22, 50]. Wang et al. [70] combined the meta-level algorithm LA-MCTS with TURBO to improve optimization performance by learning a hierarchical space partition.

In Sect. 4 we evaluate the performances of TURBO, SAASBO, ALEBO, and HESBO. Moreover, we study the popular CMA-ES [26] and random search [4].

3 The BAXUS algorithm

Wang et al. [71] showed that the REMBO embedding contains an optimum in the target space with probability one if $d \geq d_e$ and if there are no bounds on the target and input spaces, i.e., $\mathcal{Y} = \mathbb{R}^d$ and $\mathcal{X} = \mathbb{R}^D$. For $d < d_e$, it is in general impossible to represent an optimum in \mathcal{X} for arbitrary f because S projects to a d -dimensional subspace in \mathcal{X} . We call the probability of a target space to contain the optimum the *success probability*. For $d \geq d_e$, there is a positive success probability that increases with d [40, 71]. The main problem is to set d sufficiently small to avoid the detrimental effects of the curse of dimensionality, while keeping it as large as necessary to achieve a high probability that \mathcal{Y} contains an optimum.

In practice, the active subspace and its dimensionality are usually unknown. The performance of methods such as REMBO [71], HESBO [50], and ALEBO [40] depends on choosing d such that the success probability is high. Therefore, they implicitly rely on guessing the effective dimensionality d_e appropriately. We argue that choosing the target dimensionality is problematic in many practical applications. If chosen too small, the subspace cannot represent f sufficiently well. If it is chosen too large, the curse of dimensionality slows down the optimization.

The proposed algorithm, BAXUS, operates on target spaces of increasing dimensionality while preserving previous observations. Let d_{init} be the initial target dimensionality and m the total evaluation budget. BAXUS starts with a d_{init} -dimensional embedding that is increased over time until, after $m_D \leq m$ evaluations, it roughly reaches the input dimensionality D . With this strategy, we can leverage the efficiency of BO in low-dimensional spaces while guaranteeing to find an optimum in the limit. Increasing the target dimensionality is enabled by a novel embedding, which lets us carry over observations from previous, lower-dimensional target spaces into more high-dimensional target spaces. We further use a TR-based approach based on Eriksson et al. [22] to carry out optimization for high target dimensions effectively. BAXUS uses a GP surrogate [73] to model the function in the target space. Algorithm 1 gives the pseudocode for BAXUS. In Appendix B, we prove global convergence for BAXUS. We will now present the different components in detail.

Algorithm 1 BAXUS

Input: b : new bins per dimension split, D : input dimension, m_D : # evaluations by which the input dimension is reached.

Output: minimizer $\mathbf{x}^* \in \arg \min_{\mathbf{x} \in \mathcal{X}} f(\mathbf{x})$.

- 1: $d_0 \leftarrow$ initial target dimensionality of the subspace given by Eq. (3).
- 2: Compute initial projection matrix $S^\top : \mathcal{Y} \rightarrow \mathcal{X}$ by BAXUS embedding for D and d_0 .
- 3: Sample initial data $\mathcal{D} = \{(\mathbf{y}_1, f(S^\top \mathbf{y}_1)), \dots\}$ and fit the GP surrogate.
- 4: $n \leftarrow 0$
- 5: **while** evaluation budget not exhausted **do**
- 6: $L \leftarrow L_{\text{init}}$ ▷ Initialize the trust region
- 7: Calculate number of accepted “failures” as described in Sec. 3.4: $\tau_{\text{fail}}^s \leftarrow \max\left(1, \min\left(\left\lfloor \frac{m_i^s}{k} \right\rfloor, d_n\right)\right)$
- 8: **while** $L > \bar{L}_{\text{min}}$ **and** evaluation budget not exhausted **do**
- 9: Find \mathbf{y} by Thompson sampling in TR, evaluate $f(S^\top \mathbf{y})$, and add to \mathcal{D} .
- 10: Re-fit the GP hyperparameters.
- 11: Adjust trust region, see Section 3.2 for details.
- 12: **if** $d_n < D$ **then**
- 13: $d_{n+1} \leftarrow \min(d_n \cdot (b + 1), D)$.
- 14: Increase S^\top by Algorithm 2. ▷ See Appendix D
- 15: **else**
- 16: Re-sample initial data and discard previous observations, $d_{n+1} \leftarrow d_n$.
- 17: $n \leftarrow n + 1$
- 18: **Return** $S^\top(\arg \min_{\mathbf{y} \in \mathcal{D}} f(S^\top \mathbf{y}))$ or $S^\top(\arg \min_{\mathbf{y} \in \mathcal{D}} \mathbb{E}_n[f(S^\top \mathbf{y})])$. ▷ Return the best observation in case of observations without noise, or the best point according to posterior mean in case of noisy observations.

3.1 The sparse BAXUS subspace embedding

The BAXUS embedding uses a sparse projection matrix to map from \mathcal{Y} to \mathcal{X} . The number of non-zero entries in this matrix is equal to the input dimensionality D . Another embedding with this property is the HESBO embedding [50]. Given the D and a target dimensionality d , HESBO samples a target dimension in $\{1, \dots, d\}$ and a sign $\{\pm 1\}$ for each input dimension uniformly at random. Conversely, each target dimension has a set of signed contributing input dimensions. We call the set of contributing input dimensions to a target dimension a *bin*. These relations implicitly define the embedding matrix $S \in \{0, \pm 1\}^{d \times D}$, where each column has exactly one non-zero entry [15]. In the HESBO embedding, the number of contributing input dimensions varies between 0 and D .

The interpretation of contributing input dimensions allows for an intuitive way to refine the embedding, which is shown in Figure 1. We update the embedding matrix such that contributing input dimensions of the target dimension are re-assigned to the current bin and b new bins. We then say that we *split* the corresponding target dimension. Importantly, this type of embedding allows for retaining observations (see Figure 1). Assume for example, that y_i is the dimension to be split. The contributing input dimensions are re-assigned to y_i and three new target dimensions y_j, y_k , and y_l (here, $b = 3$); the observations can be retained by copying the value of the coordinate y_i to the coordinates y_j, y_k , and y_l . Thus, the observations are contained in the old and in the new target space. Algorithm 2 describes the procedure in detail.

In the BAXUS embedding, we force each bin of a target dimension to have roughly the same number of contributing input dimensions: the bin sizes differ by at most one. First, we create a random permutation of the input dimensions $1, \dots, D$. The list of input dimensions is split into $\min(d, D)$ individual bins. If d does not divide D , not all bins can have the same size. We split the permutation of input dimensions such that the i -th bin has size $\lceil D/d \rceil$, if $i + d \lfloor D/d \rfloor \leq D$, and $\lfloor D/d \rfloor$ otherwise. The first bins have one additional element with this construction if d does not divide D . We further randomly assign a sign to each input dimension. The sign of the input dimensions and their assignment to target dimensions then implicitly define S^\top (see Figure 1). We now show that the BAXUS embedding has a strictly larger worst-case success probability than the HESBO embedding. We establish the following two definitions.

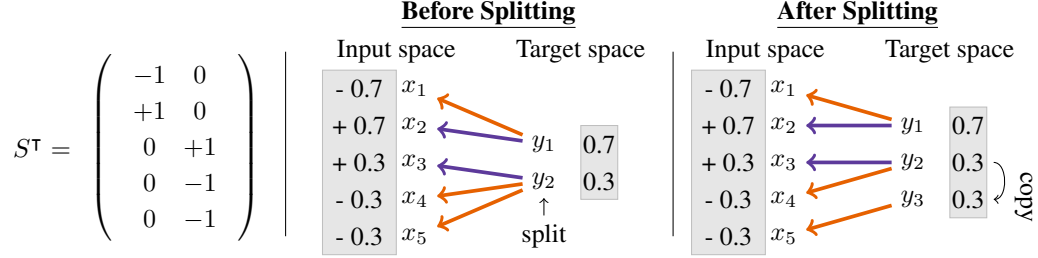


Figure 1: Observations are kept when increasing the target dimensionality. We give an example of the splitting method for $D = 5$ and $d = 2$. The first target dimension y_1 has two contributing input dimensions, x_1 and x_2 . y_2 has three contributing input dimensions, x_3 , x_4 , and x_5 . By S^T , a point $(0.7, 0.3)^T$ in the target space is mapped to $(-0.7, +0.7, +0.3, -0.3, -0.3)^T$ in the input space. Assigning the fifth input dimension to a new target dimension and copying the function values from the second target dimension does not change the observation in the input space. The new S^T is not shown but has one additional column with -1 in the last row, and the last row of the second column is set to 0.

Definition 1 (Sparse embedding matrix). A matrix $S \in \{0, \pm 1\}^{d \times D}$ is a *sparse embedding matrix* if and only if each column in S has exactly one non-zero entry [74].

We formalize the event of “recovering an optimum” [40] as follows.

Definition 2 (Success of a sparse embedding). A success of a random sparse embedding is the event $Y^* =$ “All d_e active input dimensions are mapped to distinct target dimensions.”

It is important to note that the definition of a success is sufficient but not necessary for the embedding to contain a global optimum. For example, if the origin is a global optimum, then both embeddings contain it with probability one. In that sense, the above definition provides a *worst-case guarantee*. We refer to Definition 4 in Appendix A for a formal definition of a sparse function. In Theorem 1, we give the worst-case success probability of the BAXUS embedding. All proofs have been deferred to Appendix A. Note that other than in the count-sketch algorithm [15], our hashing function is not pairwise independent. However, this does not affect our theoretical analysis.

Theorem 1 (Worst-case success probability of the BAXUS embedding). *Let D be the input dimensionality and $d \geq d_e$ the dimensionality of the embedding. Let $\beta_{small} = \lfloor \frac{D}{d} \rfloor$ and $\beta_{large} = \lceil \frac{D}{d} \rceil$ be the small and large bin sizes. Then the probability of Y^* (see Definition 2) for the BAXUS embedding is*

$$p_B(Y^*; D, d, d_e) = \frac{\sum_{i=0}^{d_e} \binom{d(1+\beta_{small})-D}{i} \binom{D-d\beta_{small}}{d_e-i} \beta_{small}^i \beta_{large}^{d_e-i}}{\binom{D}{d_e}}. \quad (1)$$

Figure 2 shows the worst-case success probabilities of the BAXUS and HESBO embeddings for three different settings of D . The worst-case success probability of the HESBO embedding is given by $p_H(Y^*; d, d_e) = d! / ((d - d_e)! d^{d_e})$ (see [40] and Appendix A.3). It is independent of D but is shown for varying d -ranges on the x -axis, therefore the probabilities seem to change between the different subplots. The BAXUS embedding ensures that the worst-case success probability is one for $d = D$. Discontinuities in the curve of the BAXUS embedding occur due to the unequal bin sizes in the BAXUS embedding’s worst-case success probability. The difference between the two embeddings in Figure 2 is particularly striking when d_e is high: for example, for $d_e = 20$ HESBO requires $d = 1000$ to reach a worst-case success probability of approximately 0.8, whereas the BAXUS embedding has a success probability of 1 as soon as $d = D$. For finite D , HESBO’s worst-case success probability is smaller than BAXUS’ success probability.

Corollary 1. *For $D \rightarrow \infty$, the worst-case success probability of the BAXUS embedding is*

$$\lim_{D \rightarrow \infty} p_B(Y^*; D, d, d_e) = \frac{d!}{(d - d_e)! d^{d_e}},$$

and hence matches HESBO’s worst-case success probability $p_H(Y^; d, d_e)$.*

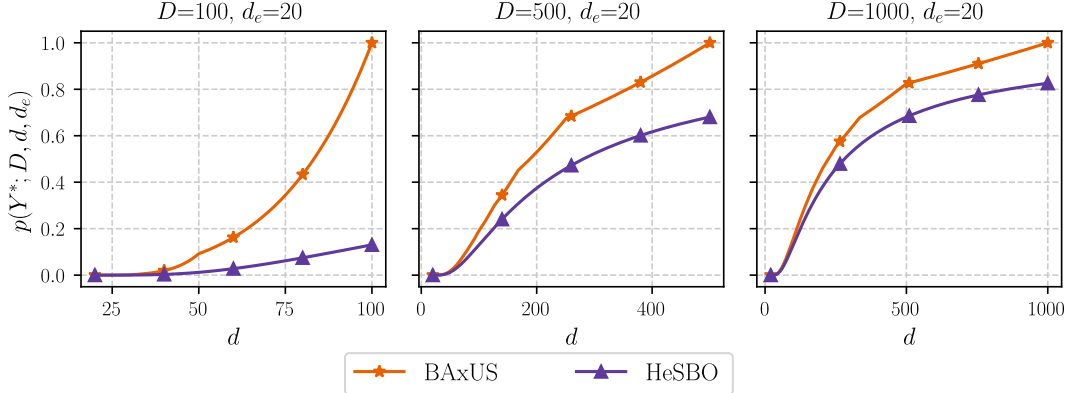


Figure 2: The worst-case guarantees for the success probabilities $p(Y^*; D, d, d_e)$ of the BAXUS and HESBO embeddings for different input dimensionalities, $D=100$ (left), $D=500$ (center), $D=1000$ (right), as a function of the target dimensionality d . The effective dimensionality is $d_e=20$. The BAXUS embedding has a higher worst-case success probability than the HESBO embedding. The improvement is large for input dimensionalities in the low hundreds and still substantial for 1000D tasks. In accordance with the theoretical analysis, the difference vanishes as the input dimension D grows.

We show that the BAXUS embedding is optimal among sparse embeddings.

Corollary 2. *With the same input, target, and effective dimensionalities (D , d , and d_e), no sparse embedding has a higher worst-case success probability than the BAXUS embedding.*

3.2 Trust-region approach

Similar to TURBO [22], BAXUS operates in trust regions (TRs). TRs are hyper-rectangles in the input space. Their shape is determined by their *base side length* L and the GP length scales. The side length for each dimension is proportional to the corresponding length scale of the GP kernel fitted to the data. The idea of this construction is that length scales indicate how quickly the function changes along the associated dimension. Thus, the TR is rescaled accordingly. The volume of a TR is shrunk when TURBO fails τ_{fail} consecutive times to make progress, i.e., to find a better solution. If the algorithm consecutively makes progress for $\tau_{\text{success}} = 3$ times, it expands the TR. It restarts when the base side length L of the current TR falls below a threshold $L_{\text{min}} := 2^{-7}$. In that case, it discards all observations for the TR and initializes a new TR on new samples. TRs enable TURBO to focus on regions of the space close to the incumbent, i.e., the current best solution found by the algorithm. To choose the next evaluation point, TURBO uses Thompson sampling [66], i.e., it draws a realization of the GP on a set of candidate locations in the TR and then selects a point of minimum sampled value.

TRs are an essential component of BAXUS because the target dimensionality usually grows exponentially during a run of the algorithm. We use the same hyperparameter settings as TURBO [22] with the following modifications. First, we change the criterion for when to restart a TR. Instead of restarting a TR when it becomes too small, we increase the target dimensionality by splitting each target dimension into several new bins unless BAXUS has already reached the input dimensionality. In this case, we reset the TR base side length to the initial value and re-initialize the algorithm with a new random set of initial observations. By resetting the base side length, we also avoid convergence to a particular local minimum as the TR covers large regions of the space again. TURBO solves this problem by allowing for multiple parallel TRs. Secondly, we change the number of accepted “failures” τ_{fail} , such that BAXUS can roughly reach the input dimensionality in a fixed number of evaluations as described in Section 3.4.

3.3 Splitting strategy

Starting in a low-dimensional embedded space, BAXUS successively grows the target dimensionality to increase the probability of containing an optimum. By Corollary 2, it is optimal to keep the number

of contributing input dimensions in the target bins as equal as possible. At each splitting point, the target dimensionality grows exponentially. The number of splits required to reach some input dimensionality D is logarithmic in D . BAXUS uses a larger evaluation budget in each split. Suppose that the algorithm starts in target dimensionality d_{init} . Then, after k splits, the target dimensionality is $d_k = d_{\text{init}}(b + 1)^k$.

3.4 Controlling the number of accepted failures

BAXUS needs to be able to reach high target dimensionalities to find a global optimum. As described in Section 3.2, BAXUS increases the target dimensionality when the TR base side length falls below the minimum threshold. For this to happen, the TR base length needs to be halved at least $k = \left\lceil \log_{\frac{1}{2}} \frac{L_{\text{min}}}{L_{\text{init}}} \right\rceil$ times. Halving occurs if BAXUS consecutively fails τ_{fail} times in finding a better function value. If, similarly to TURBO, we set the number of accepted “failures” τ_{fail} to the current target dimensionality of the TR, we get the lower bound $k \cdot \tau_{\text{fail}}$ on the number of function evaluations spent in that target dimensionality. This bound does not scale with the input dimensionality D of the problem, i.e., the maximum target dimensionality is independent of D for a fixed evaluation budget.

To enable BAXUS to reach any desired target dimensionality for the fixed evaluation budget, we scale down τ_{fail} dependent on D , i.e., we adjust the lower bound. We choose to make it dependent on D as we are guaranteed that the target space contains all global optima if the final target space corresponds to the input space \mathcal{X} (see Appendix B). In contrast to imposing a hard limit on the number of function evaluations in a target dimensionality, scaling down the number of accepted “failures” has the advantage that we do not restrain BAXUS in cases where it finds better function values. The idea is to choose τ_{fail} dependent on the current target dimensionality d_i and such that BAXUS can reach any desired target dimensionality.

We calculate the number of splits n required to reach D by

$$D \approx d_{\text{init}} \cdot (b + 1)^n \Rightarrow n = \left\lceil \log_{b+1} \frac{D}{d_{\text{init}}} \right\rceil, \quad (2)$$

with $\lceil \cdot \rceil$ indicating rounding to the nearest integer. The minimum evaluation budget for a split is then found by multiplying m_D with the “weight” of each target dimensionality. We assign each split i a *split budget* m_i^s that is proportional to d_i , such that $\sum_{i=0}^n m_i^s = m_D$, where m_D is the budgeted number of function evaluations until D would be reached under the above assumptions:

$$m_i^s = \left\lfloor m_D \frac{d_i}{\sum_{k=0}^n d_k} \right\rfloor = \left\lfloor \frac{b \cdot m_D \cdot d_i}{d_{\text{init}}((b + 1)^{n+1} - 1)} \right\rfloor.$$

Finally, we set the number τ_{fail}^i of accepted “failures” for the i -th target dimensionality d_i such that (1) it adheres to its *split budget* in the event that it never obtains a better function value, (2) it is not larger than if we would use TURBO’s choice d_i , and (3) it is at least 1:

$$\tau_{\text{fail}}^i = \max \left(1, \min \left(\left\lfloor \frac{m_i^s}{k} \right\rfloor, d_i \right) \right).$$

Setting the initial target dimension. Due to the rounding in Eq. (2) and the exponential growth of the target dimensionality, the final target dimensionality $d_{\text{init}} \cdot (b + 1)^n$ might differ considerably from the input dimensionality D . This is undesirable as we might not reach D before depleting the evaluation budget, or we might overestimate the evaluation budget for the final target dimensionality d_n . Therefore, we set the initial target dimensionality such that the final target dimensionality is as close to D as possible:

$$d_{\text{init}} = \arg \min_{i \in \{1, \dots, b\}} |i \cdot (b + 1)^n - D|, \quad (3)$$

where n is given by Eq. (2). We point out that $1 \leq d_{\text{init}} \leq b$. An alternative to adjusting d_{init} would be to fix the initial d_0 and adjust the growth factor b .

4 Experimental evaluation

In this section, we evaluate the performance of BAXUS on a 388D hyperparameter optimization task, a 124D design problem, and a collection of tasks that exhibit an active subspace. The BAXUS code is available at <https://github.com/LeoIV/BAXUS>.

The experimental setup. We benchmark against TURBO [22] with one and five trust regions, SAASBO [20], ALEBO [40], random search [4], CMA-ES [26], and HESBO [50], using the implementations provided by the respective authors with their settings, unless stated otherwise. For CMA-ES, we use the PYCMA [27] implementation. For HESBO and ALEBO, we use the AX implementation [1]. To show the effect of different choices of d , we run HESBO and ALEBO with $d = 10$ and $d = 20$. We observed that ALEBO and SAASBO are constrained by their high runtime and memory consumption. The available hardware allowed up to 100 function evaluations for SAASBO and 500 function evaluations for ALEBO for each individual run. Larger sampling budgets or higher target dimensions for ALEBO resulted in out-of-memory errors. We point out that limited scalability was expected for these two methods, whereas the other methods scaled to considerably larger budgets, as required for scalable BO. We initialize each optimizer, including BAXUS, with ten initial samples and BAXUS with $b = 3$ and $m_D = 1000$ and run 20 repeated trials. Plots show the mean performance with one standard error.

The benchmarks. We evaluate the selected algorithms on six benchmarks that differ considerably in their characteristics. Following [71], we augment the BRANIN2 and HARTMANN6 functions with additional dummy dimensions that have no influence on the function value. We use the 388D SVM benchmark and the 124D soft-constraint version of the MOPTA08 benchmark proposed in [20]. We set a budget of 1000 evaluations for MOPTA08, BRANIN2, and HARTMANN6 and of 2000 evaluations for the other benchmarks. Moreover, we stopped for BRANIN2 and HARTMANN6 when the simple regret dropped below .001. We show results on additional noise-free benchmarks in Appendices C.2 and C.3. We also tested the algorithms on the 300D LASSO-HIGH and the 1000D LASSO-HARD benchmarks from LASSOBENCH [59]. These benchmarks have an effective dimensionality of 5% of the input dimensionality, i.e., the LASSO-HIGH and LASSO-HARD benchmarks have 15 and 50 effective dimensions, respectively. To study the robustness to observational noise, we also tested on noisy variants of LASSO-HARD and LASSO-HIGH.

4.1 Experimental results

We begin with the six noise-free benchmarks. Fig. 3 summarizes the performances. On MOPTA08, a 124D vehicle design problem, SAASBO initially makes slightly faster progress than BAXUS. We suspect that this benchmark has high effective dimensionality, such that BAXUS first needs to adapt the target dimensionality to make further progress. On the 388D SVM benchmark, BAXUS adapts to the appropriate target dimensionality where it can reach good function values faster than TURBO and CMA-ES. For this benchmark, Eriksson and Jankowiak [20] reported that SAASBO learned three active dimensions. Yet, the fact that ALEBO and HESBO seem to stagnate after a few hundred evaluations, while BAXUS, TURBO, and CMA-ES find better solutions, indicates that optimizing more of the 385 kernel length scales of the SVM benchmark allows for better solutions. On the 500D HARTMANN6, SAASBO performs best, closely followed by BAXUS. ALEBO and HESBO are competitive initially but converge to suboptimal solutions. HESBO, BAXUS, SAASBO, ALEBO all find excellent solutions on the BRANIN benchmark, with the latter algorithms converging faster.

Next, we examine the performances on the 1000D LASSO-HARD and the 300D LASSO-HIGH that exhibit active subspaces, here without observational noise. BAXUS achieves considerably better solutions than all state-of-the-art methods. We also note that TURBO and CMA-ES perform better than SAASBO and ALEBO. While one may expect BAXUS to outperform TURBO and CMA-ES on these tasks with high input dimensions, it is surprising that SAASBO, HESBO, and ALEBO are not able to benefit from the present active subspace. Here BAXUS’s strategy to adaptively expand the nested subspace is superior. Another crucial observation is that performances of BAXUS vary only slightly across runs. Thus, BAXUS is robust despite the stochastic construction of the embedding. Across the broad collection of benchmarks, BAXUS is the only method to consistently achieve high performance.

Noisy benchmarks. We evaluate the algorithms also for tasks with observational noise. Fig. 4 summarizes the results. We observe that BAXUS achieves considerably better solutions for any number of observations than the competitors. Moreover, we note that the performances of SAASBO, CMA-ES, and HESBO ($d = 20$) degrade considerably on the LASSO-HIGH task compared to the noise-free formulation of the task studied above. BAXUS’ performance is equally strong as for the noise-free case and keeps making progress after 1000 observations.

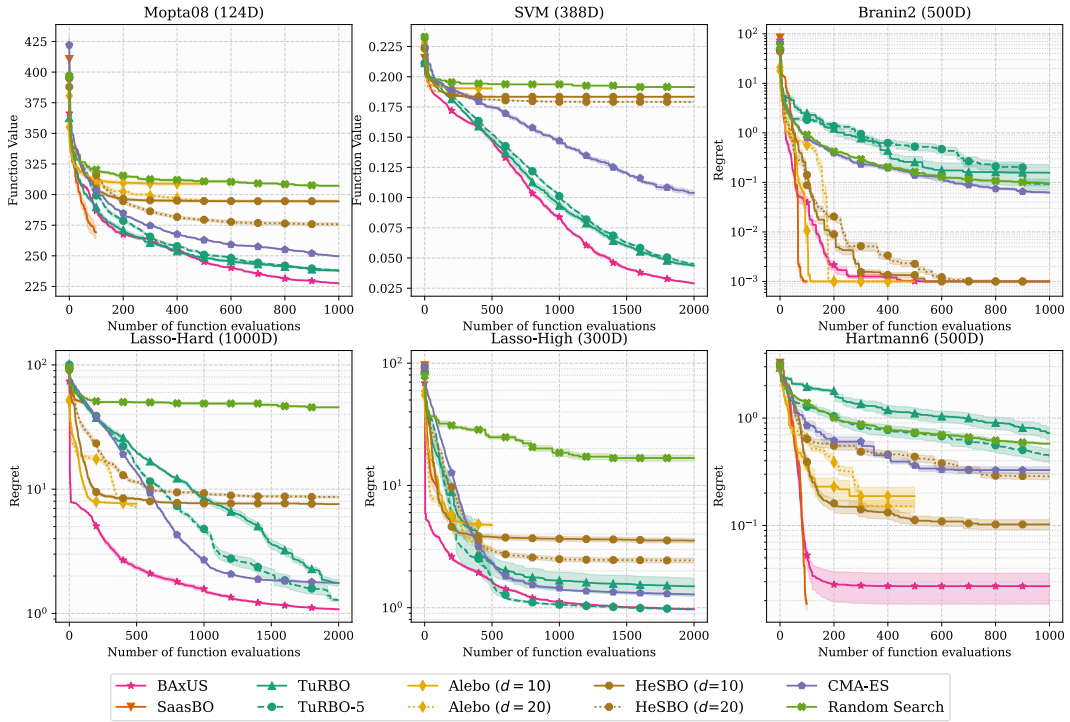


Figure 3: Top row: **124D MOPTA08 (l)**: BAXUS obtains the best solutions, followed by TuRBO and CMA-ES. **388D SVM (c)**: BAXUS outperforms the other methods from the start. **500D BRANIN (r)**: SAASBO, BAXUS, ALEBO, and HESBO find an optimum; SAASBO and ALEBO converge fastest. Bottom row: **100D LASSO-HARD (l)** and **300D LASSO-HIGH (c)**: BAXUS outperforms the baselines. SAASBO, ALEBO, and HESBO struggle. **500D HARTMANN6 (r)**: SAASBO performs best, closely followed by BAXUS. The other methods show only slow progress or stagnate.

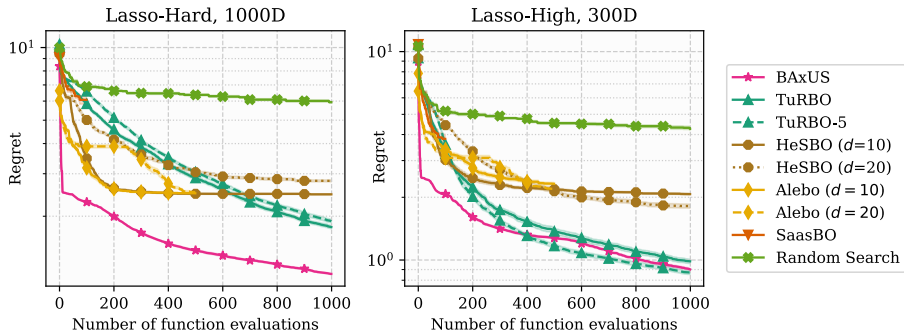


Figure 4: BAXUS outperforms the SOTA and in particular proves to be robust to observational noise on the **1000D LASSO-HARD (l)** and the **300D LASSO-HIGH (r)**. Note that CMA-ES performs considerably worse than on the noise-free versions of the benchmarks.

BAXUS embedding ablation study. To investigate whether the proposed family of nested random subspaces contributes to the superior performance of BAXUS, we replaced the new embedding with a similar family of nested HESBO embeddings. The results show that the proposed embedding provides a significant performance gain. Due to space constraints, the results were moved to Appendix C.1.

5 Discussion

High-dimensional Bayesian optimization is aspiring to unlock impactful applications broadly in science and industry. However, state-of-the-art methods suffer from limited scalability or, in some cases, require practitioners to ‘guess’ certain hyperparameters that critically impact the performance. This paper proposes BAXUS that works out-of-the-box and achieves considerably better performance for high-dimensional problems, as the comprehensive evaluation shows. A key idea is to scale up the dimensionality of the target subspace that the algorithm optimizes over. We apply a simple strategy that we find to work well across the board. However, we expect substantial headroom in tailoring this strategy to specific applications, either using domain expertise or a more sophisticated data-driven approach that, for example, learns a suitable target space. Moreover, future work will explore extending BAXUS to structured domains, particularly the combinatorial spaces common in materials sciences and drug discovery.

Societal impact. Bayesian optimization has recently become a popular tool for tasks in drug discovery [51], chemical engineering [11, 28, 31, 58, 60], materials science [23, 29, 30, 52, 64, 68], aerospace engineering [2, 39, 43], robotics [12, 13, 41, 46, 54], and many more. This speaks to the progress that Bayesian optimization has made in becoming a robust and reliable ‘off-the-shelf solver.’ However, this promise is not yet fulfilled for the newer field of high-dimensional Bayesian optimization that allows optimization over hundreds of ‘tunable levers.’ The abovementioned applications benefit from incorporating more such levers in the optimization: it allows for more detailed modeling of an aerospace design or a more granular control of a chemical reaction, to give some examples. The evaluation shows that the performance of state-of-the-art methods degenerates drastically for such high dimensions if the application does not meet specific requirements. Adding insult to the injury, such requirements as the dimensionality of an active subspace cannot be determined beforehand.

The proposed algorithm achieves a robust performance over a broad collection of tasks and thus will become a ‘goto’ optimizer for practitioners in other fields. Therefore, we released the BAXUS code.

Acknowledgments and Disclosure of Funding

Luigi Nardi was supported in part by affiliate members and other supporters of the Stanford DAWN project — Ant Financial, Facebook, Google, Intel, Microsoft, NEC, SAP, Teradata, and VMware. Leonard Papenmeier and Luigi Nardi were partially supported by the Wallenberg AI, Autonomous Systems and Software Program (WASP) funded by the Knut and Alice Wallenberg Foundation. Luigi Nardi was partially supported by the Wallenberg Launch Pad (WALP) grant Dnr 2021.0348. The computations were also enabled by resources provided by the Swedish National Infrastructure for Computing (SNIC) at LUNARC, partially funded by the Swedish Research Council through grant agreement no. 2018-05973. We would like to thank Erik Hellsten from Lund University and Eddy de Weerd from the University of Twente for valuable discussions.

References

- [1] E. Bakshy, L. Dworkin, B. Karrer, K. Kashin, B. Letham, A. Murthy, and S. Singh. Ae: A domain-agnostic platform for adaptive experimentation. In *Conference on Neural Information Processing Systems*, pages 1–8, 2018.
- [2] R. Baptista and M. Poloczek. Bayesian optimization of combinatorial structures. In *International Conference on Machine Learning*, pages 462–471. PMLR, 2018.
- [3] E. F. Beckenbach and R. Bellman. *Inequalities*, volume 30. Springer Science & Business Media, 2012.
- [4] J. Bergstra and Y. Bengio. Random search for hyper-parameter optimization. *Journal of machine learning research*, 13(2), 2012.
- [5] J. Bergstra, R. Bardenet, Y. Bengio, and B. Kégl. Algorithms for Hyper-Parameter Optimization. In *Advances in Neural Information Processing Systems (NeurIPS)*, volume 24. Curran Associates, Inc., 2011.
- [6] M. Binois. *Uncertainty quantification on Pareto fronts and high-dimensional strategies in Bayesian optimization, with applications in multi-objective automotive design*. PhD thesis, Ecole Nationale Supérieure des Mines de Saint-Etienne, 2015.
- [7] M. Binois and N. Wycoff. A survey on high-dimensional Gaussian process modeling with application to Bayesian optimization. *ACM Transactions on Evolutionary Learning and Optimization*, 2(2):1–26, 2022.
- [8] M. Binois, D. Ginsbourger, and O. Roustant. A warped kernel improving robustness in Bayesian optimization via random embeddings. In *International Conference on Learning and Intelligent Optimization (LION)*, pages 281–286. Springer, 2015.
- [9] M. Binois, D. Ginsbourger, and O. Roustant. On the choice of the low-dimensional domain for global optimization via random embeddings. *Journal of global optimization*, 76(1):69–90, 2020.
- [10] M. A. Bouhlel, N. Bartoli, R. G. Regis, A. Otsmane, and J. Morlier. Efficient global optimization for high-dimensional constrained problems by using the Kriging models combined with the partial least squares method. *Engineering Optimization*, 50(12):2038–2053, 2018.
- [11] B. Burger, P. M. Maffettone, V. V. Gusev, C. M. Aitchison, Y. Bai, X. Wang, X. Li, B. M. Alston, B. Li, R. Clowes, et al. A mobile robotic chemist. *Nature*, 583(7815):237–241, 2020.
- [12] R. Calandra, N. Gopalan, A. Seyfarth, J. Peters, and M. P. Deisenroth. Bayesian Gait Optimization for Bipedal Locomotion. In P. M. Pardalos, M. G. Resende, C. Vogiatzis, and J. L. Walteros, editors, *Learning and Intelligent Optimization*, pages 274–290, Cham, 2014. Springer International Publishing.
- [13] R. Calandra, A. Seyfarth, J. Peters, and M. P. Deisenroth. Bayesian optimization for learning gaits under uncertainty. *Annals of Mathematics and Artificial Intelligence*, 76(1):5–23, 2016.
- [14] A. Candelieri, R. Perego, and F. Archetti. Bayesian Optimization of Pump Operations in Water Distribution Systems. *Journal of Global Optimization*, 71(1):213–235, May 2018. ISSN 0925-5001.
- [15] M. Charikar, K. Chen, and M. Farach-Colton. Finding Frequent Items in Data Streams. In P. Widmayer, S. Eidenbenz, F. Triguero, R. Morales, R. Conejo, and M. Hennessy, editors, *Automata, Languages and Programming*, pages 693–703, Berlin, Heidelberg, 2002. Springer Berlin Heidelberg. ISBN 978-3-540-45465-6.
- [16] J. Chen, G. Zhu, C. Yuan, and Y. Huang. Semi-supervised Embedding Learning for High-dimensional Bayesian Optimization. *arXiv preprint arXiv:2005.14601*, 2020.
- [17] P. G. Constantine. *Active Subspaces*. Society for Industrial and Applied Mathematics, Philadelphia, PA, 2015.

- [18] Z. Cosenza, R. Astudillo, P. Frazier, K. Baar, and D. E. Block. Multi-Information Source Bayesian Optimization of Culture Media for Cellular Agriculture. *Biotechnology and Bioengineering*, 2022.
- [19] A. Ejje, L. Medvinsky, A. Councilman, H. Nehra, S. Sharma, V. Adve, L. Nardi, E. Nurvitadhi, and R. A. Rutenbar. HPVM2FPGA: Enabling True Hardware-Agnostic FPGA Programming. In *Proceedings of the 33rd IEEE International Conference on Application-specific Systems, Architectures, and Processors*, 2022.
- [20] D. Eriksson and M. Jankowiak. High-dimensional Bayesian optimization with sparse axis-aligned subspaces. In C. de Campos and M. H. Maathuis, editors, *Proceedings of the Thirty-Seventh Conference on Uncertainty in Artificial Intelligence*, volume 161 of *Proceedings of Machine Learning Research*, pages 493–503. PMLR, 27–30 Jul 2021.
- [21] D. Eriksson and M. Poloczek. Scalable Constrained Bayesian Optimization. In A. Banerjee and K. Fukumizu, editors, *Proceedings of The 24th International Conference on Artificial Intelligence and Statistics*, volume 130 of *Proceedings of Machine Learning Research*, pages 730–738. PMLR, 13–15 Apr 2021.
- [22] D. Eriksson, M. Pearce, J. Gardner, R. D. Turner, and M. Poloczek. Scalable Global Optimization via Local Bayesian Optimization. In *Advances in Neural Information Processing Systems (NeurIPS)*, pages 5496–5507, 2019.
- [23] P. I. Frazier and J. Wang. *Bayesian Optimization for Materials Design*, pages 45–75. Springer International Publishing, Cham, 2016. ISBN 978-3-319-23871-5.
- [24] J. Gardner, C. Guo, K. Weinberger, R. Garnett, and R. Grosse. Discovering and exploiting additive structure for Bayesian optimization. In *International Conference on Artificial Intelligence and Statistics*, pages 1311–1319, 2017.
- [25] R. L. Graham, D. E. Knuth, O. Patashnik, and S. Liu. Concrete mathematics: a foundation for computer science. *Computers in Physics*, 3(5):106–107, 1989.
- [26] N. Hansen and A. Ostermeier. Adapting arbitrary normal mutation distributions in evolution strategies: the covariance matrix adaptation. In *Proceedings of IEEE International Conference on Evolutionary Computation (ICEC)*, pages 312–317, 1996.
- [27] N. Hansen, Y. Akimoto, and P. Baudis. CMA-ES/pycma on Github. Zenodo, DOI:10.5281/zenodo.2559634, Feb. 2019. Last accessed: 05/09/2022. License: BSD-3-Clause.
- [28] F. Hase, L. M. Roch, C. Kreisbeck, and A. Aspuru-Guzik. Phoenix: a Bayesian optimizer for chemistry. *ACS central science*, 4(9):1134–1145, 2018.
- [29] F. Häse, M. Aldeghi, R. J. Hickman, L. M. Roch, and A. Aspuru-Guzik. Gryffin: An algorithm for Bayesian optimization of categorical variables informed by expert knowledge. *Applied Physics Reviews*, 8(3):031406, 2021.
- [30] H. C. Herbol, W. Hu, P. Frazier, P. Clancy, and M. Poloczek. Efficient search of compositional space for hybrid organic–inorganic perovskites via Bayesian optimization. *npj Computational Materials*, 4(1):1–7, 2018.
- [31] J. M. Hernández-Lobato, J. Requeima, E. O. Pyzer-Knapp, and A. Aspuru-Guzik. Parallel and Distributed Thompson Sampling for Large-scale Accelerated Exploration of Chemical Space. In *Proceedings of the 34th International Conference on Machine Learning*, volume 70 of *Proceedings of Machine Learning Research*, pages 1470–1479. PMLR, 06–11 Aug 2017.
- [32] Z. E. Hughes, M. A. Nguyen, J. Wang, Y. Liu, M. T. Swihart, M. Poloczek, P. I. Frazier, M. R. Knecht, and T. R. Walsh. Tuning materials-binding peptide sequences toward gold- and silver-binding selectivity with Bayesian optimization. *ACS nano*, 15(11):18260–18269, 2021.
- [33] C. Hvarfner, D. Stoll, A. Souza, L. Nardi, M. Lindauer, and F. Hutter. PiBO: Augmenting Acquisition Functions with User Beliefs for Bayesian Optimization. In *International Conference on Learning Representations*, 2022.

- [34] D. R. Jones. Large-scale multi-disciplinary mass optimization in the auto industry. In *MOPTA 2008 Conference (20 August 2008)*, 2008.
- [35] K. Kandasamy, J. Schneider, and B. Póczos. High dimensional Bayesian optimisation and bandits via additive models. In *International conference on machine learning (ICML)*, pages 295–304, 2015.
- [36] K. Kandasamy, W. Neiswanger, J. Schneider, B. Póczos, and E. P. Xing. Neural Architecture Search with Bayesian Optimisation and Optimal Transport. In S. Bengio, H. Wallach, H. Larochelle, K. Grauman, N. Cesa-Bianchi, and R. Garnett, editors, *Advances in Neural Information Processing Systems (NeurIPS)*, volume 31. Curran Associates, Inc., 2018.
- [37] D. P. Kingma and M. Welling. Auto-Encoding Variational Bayes. In *2nd International Conference on Learning Representations, ICLR 2014, Banff, AB, Canada, April 14-16, 2014, Conference Track Proceedings*, 2014.
- [38] A. Klein, S. Falkner, S. Bartels, P. Hennig, and F. Hutter. Fast Bayesian Optimization of Machine Learning Hyperparameters on Large Datasets. In A. Singh and J. Zhu, editors, *Proceedings of the 20th International Conference on Artificial Intelligence and Statistics*, volume 54 of *Proceedings of Machine Learning Research*, pages 528–536. PMLR, 20–22 Apr 2017.
- [39] R. Lam, M. Poloczek, P. Frazier, and K. E. Willcox. Advances in Bayesian optimization with applications in aerospace engineering. In *2018 AIAA Non-Deterministic Approaches Conference*, page 1656, 2018.
- [40] B. Letham, R. Calandra, A. Rai, and E. Bakshy. Re-Examining Linear Embeddings for High-Dimensional Bayesian Optimization. In *Advances in Neural Information Processing Systems (NeurIPS)*, volume 33, pages 1546–1558. Curran Associates, Inc., 2020.
- [41] D. J. Lizotte, T. Wang, M. H. Bowling, D. Schuurmans, et al. Automatic Gait Optimization With Gaussian Process Regression. In *IJCAI*, volume 7, pages 944–949, 2007.
- [42] X. Lu, J. Gonzalez, Z. Dai, and N. D. Lawrence. Structured Variationally Auto-encoded Optimization. In J. G. Dy and A. Krause, editors, *Proceedings of the 35th International Conference on Machine Learning, ICML 2018, Stockholmsmässan, Stockholm, Sweden, July 10-15, 2018*, volume 80 of *Proceedings of Machine Learning Research*, pages 3273–3281. PMLR, 2018.
- [43] T. W. Lukaczyk, P. Constantine, F. Palacios, and J. J. Alonso. Active subspaces for shape optimization. In *10th AIAA multidisciplinary design optimization conference*, page 1171, 2014.
- [44] A. W. Marshall, I. Olkin, and B. C. Arnold. *Inequalities: theory of majorization and its applications*, volume 143. Springer, 1979.
- [45] N. Maus, H. T. Jones, J. Moore, M. Kusner, J. Bradshaw, and J. R. Gardner. Local latent space bayesian optimization over structured inputs. In *Advances in Neural Information Processing Systems*, 2022.
- [46] M. Mayr, F. Ahmad, K. I. Chatzilygeroudis, L. Nardi, and V. Krüger. Skill-based Multi-objective Reinforcement Learning of Industrial Robot Tasks with Planning and Knowledge Integration. *CoRR*, abs/2203.10033, 2022.
- [47] R. Moriconi, M. P. Deisenroth, and K. S. Sesh Kumar. High-dimensional Bayesian optimization using low-dimensional feature spaces. *Machine Learning*, 109(9):1925–1943, Sep 2020. ISSN 1573-0565.
- [48] M. Mutny and A. Krause. Efficient high dimensional Bayesian optimization with additivity and quadrature Fourier features. *Advances in Neural Information Processing Systems*, 31, 2018.
- [49] L. Nardi, D. Koeplinger, and K. Olukotun. Practical design space exploration. In *2019 IEEE 27th International Symposium on Modeling, Analysis, and Simulation of Computer and Telecommunication Systems (MASCOTS)*, pages 347–358. IEEE, 2019.

- [50] A. Nayebi, A. Munteanu, and M. Poloczek. A framework for Bayesian Optimization in Embedded Subspaces. In K. Chaudhuri and R. Salakhutdinov, editors, *Proceedings of the 36th International Conference on Machine Learning*, volume 97 of *Proceedings of Machine Learning Research (PMLR)*, pages 4752–4761. PMLR, 09–15 Jun 2019.
- [51] D. M. Negoescu, P. I. Frazier, and W. B. Powell. The Knowledge-Gradient Algorithm for Sequencing Experiments in Drug Discovery. *INFORMS Journal on Computing*, 23(3):346–363, 2011.
- [52] D. Packwood. *Bayesian Optimization for Materials Science*. Springer, 2017.
- [53] G. Pedrielli and S. H. Ng. G-STAR: A new kriging-based trust region method for global optimization. In *2016 Winter Simulation Conference (WSC)*, pages 803–814. IEEE, 2016.
- [54] A. Rai, R. Antonova, S. Song, W. Martin, H. Geyer, and C. Atkeson. Bayesian optimization using domain knowledge on the ATRIAS biped. In *2018 IEEE International Conference on Robotics and Automation (ICRA)*, pages 1771–1778. IEEE, 2018.
- [55] R. G. Regis. Trust regions in Kriging-based optimization with expected improvement. *Engineering optimization*, 48(6):1037–1059, 2016.
- [56] H. Robbins. A remark on stirling’s formula. *The American mathematical monthly*, 62(1):26–29, 1955.
- [57] B. Ru, X. Wan, X. Dong, and M. Osborne. Interpretable Neural Architecture Search via Bayesian Optimisation with Weisfeiler-Lehman Kernels. In *International Conference on Learning Representations*, 2021.
- [58] A. M. Schweidtmann, A. D. Clayton, N. Holmes, E. Bradford, R. A. Bourne, and A. A. Lapkin. Machine learning meets continuous flow chemistry: Automated optimization towards the Pareto front of multiple objectives. *Chemical Engineering Journal*, 352:277–282, 2018.
- [59] K. Šehić, A. Gramfort, J. Salmon, and L. Nardi. LassoBench: A High-Dimensional Hyperparameter Optimization Benchmark Suite for Lasso. In *First Conference on Automated Machine Learning (Main Track)*, 2022.
- [60] B. J. Shields, J. Stevens, J. Li, M. Parasram, F. Damani, J. I. M. Alvarado, J. M. Janey, R. P. Adams, and A. G. Doyle. Bayesian reaction optimization as a tool for chemical synthesis. *Nature*, 590(7844):89–96, 2021.
- [61] J. Snoek, H. Larochelle, and R. P. Adams. Practical Bayesian Optimization of Machine Learning Algorithms. In F. Pereira, C. Burges, L. Bottou, and K. Weinberger, editors, *Advances in Neural Information Processing Systems*, volume 25. Curran Associates, Inc., 2012.
- [62] H. H. Sohrab. *Basic real analysis*, volume 231. Springer, 2003.
- [63] F. J. Solis and R. J.-B. Wets. Minimization by Random Search Techniques. *Mathematics of Operations Research*, 6(1):19–30, 1981. ISSN 0364765X, 15265471.
- [64] A. Souza, L. B. Oliveira, S. Hollatz, M. Feldman, K. Olukotun, J. M. Holton, A. E. Cohen, and L. Nardi. DeepFreak: Learning crystallography diffraction patterns with automated machine learning. *arXiv preprint arXiv:1904.11834*, 2019.
- [65] L. Tallorin, J. Wang, W. E. Kim, S. Sahu, N. M. Kosa, P. Yang, M. Thompson, M. K. Gilson, P. I. Frazier, M. D. Burkart, et al. Discovering de novo peptide substrates for enzymes using machine learning. *Nature communications*, 9(1):1–10, 2018.
- [66] W. R. Thompson. On the Likelihood that One Unknown Probability Exceeds Another in View of the Evidence of Two Samples. *Biometrika*, 25(3/4):285–294, 1933. ISSN 00063444.
- [67] A. Tripp, E. Daxberger, and J. M. Hernández-Lobato. Sample-Efficient Optimization in the Latent Space of Deep Generative Models via Weighted Retraining. In H. Larochelle, M. Ranzato, R. Hadsell, M. Balcan, and H. Lin, editors, *Advances in Neural Information Processing Systems (NeurIPS)*, volume 33, pages 11259–11272. Curran Associates, Inc., 2020.

- [68] T. Ueno, T. D. Rhone, Z. Hou, T. Mizoguchi, and K. Tsuda. COMBO: An efficient Bayesian optimization library for materials science. *Materials Discovery*, 4:18–21, 2016. ISSN 2352-9245.
- [69] X. Wan, V. Nguyen, H. Ha, B. Ru, C. Lu, and M. A. Osborne. Think Global and Act Local: Bayesian Optimisation over High-Dimensional Categorical and Mixed Search Spaces. In *Proceedings of the 38th International Conference on Machine Learning*, volume 139 of *Proceedings of Machine Learning Research*, pages 10663–10674. PMLR, 18–24 Jul 2021.
- [70] L. Wang, R. Fonseca, and Y. Tian. Learning Search Space Partition for Black-box Optimization using Monte Carlo Tree Search. *Advances in Neural Information Processing Systems*, 33: 19511–19522, 2020.
- [71] Z. Wang, F. Hutter, M. Zoghi, D. Matheson, and N. de Freitas. Bayesian optimization in a billion dimensions via random embeddings. *Journal of Artificial Intelligence Research (JAIR)*, 55: 361–387, 2016.
- [72] Z. Wang, C. Gehring, P. Kohli, and S. Jegelka. Batched large-scale Bayesian optimization in high-dimensional spaces. In *International Conference on Artificial Intelligence and Statistics*, pages 745–754, 2018.
- [73] C. K. Williams and C. E. Rasmussen. *Gaussian processes for machine learning*, volume 2. MIT press Cambridge, MA, 2006.
- [74] D. P. Woodruff et al. Sketching as a tool for numerical linear algebra. *Foundations and Trends® in Theoretical Computer Science*, 10(1–2):1–157, 2014.
- [75] J. Zhou, Z. Yang, Y. Si, L. Kang, H. Li, M. Wang, and Z. Zhang. A trust-region parallel Bayesian optimization method for simulation-driven antenna design. *IEEE Transactions on Antennas and Propagation*, 69(7):3966–3981, 2020.

Checklist

1. For all authors...
 - (a) Do the main claims made in the abstract and introduction accurately reflect the paper's contributions and scope? [Yes]
 - (b) Did you describe the limitations of your work? [Yes] See Section 5.
 - (c) Did you discuss any potential negative societal impacts of your work? [Yes] See Section 5.
 - (d) Have you read the ethics review guidelines and ensured that your paper conforms to them? [Yes]
2. If you are including theoretical results...
 - (a) Did you state the full set of assumptions of all theoretical results? [Yes]
 - (b) Did you include complete proofs of all theoretical results? [Yes] See Appendix A.
3. If you ran experiments...
 - (a) Did you include the code, data, and instructions needed to reproduce the main experimental results (either in the supplemental material or as a URL)? [Yes]
 - (b) Did you specify all the training details (e.g., data splits, hyperparameters, how they were chosen)? [Yes]
 - (c) Did you report error bars (e.g., with respect to the random seed after running experiments multiple times)? [Yes]
 - (d) Did you include the total amount of compute and the type of resources used (e.g., type of GPUs, internal cluster, or cloud provider)? [Yes] See Appendix E.
4. If you are using existing assets (e.g., code, data, models) or curating/releasing new assets...
 - (a) If your work uses existing assets, did you cite the creators? [Yes] See Appendix E.
 - (b) Did you mention the license of the assets? [Yes] See Appendix E.
 - (c) Did you include any new assets either in the supplemental material or as a URL? [Yes]
 - (d) Did you discuss whether and how consent was obtained from people whose data you're using/curating? [N/A]
 - (e) Did you discuss whether the data you are using/curating contains personally identifiable information or offensive content? [N/A]
5. If you used crowdsourcing or conducted research with human subjects...
 - (a) Did you include the full text of instructions given to participants and screenshots, if applicable? [N/A]
 - (b) Did you describe any potential participant risks, with links to Institutional Review Board (IRB) approvals, if applicable? [N/A]
 - (c) Did you include the estimated hourly wage paid to participants and the total amount spent on participant compensation? [N/A]

A Theoretical foundation for the BAXUS embedding

For convenience, we re-state Definition 1 and Definition 2 from Section 3.

Definition 1 (Sparse embedding matrix). A matrix $S \in \{0, \pm 1\}^{d \times D}$ is a *sparse embedding matrix* if and only if each column in S has exactly one non-zero entry [74].

Definition 2 (Success of a sparse embedding). A success of a random sparse embedding is the event $Y^* =$ “All d_e active input dimensions are mapped to distinct target dimensions.”

We introduce the following two definitions.

Definition 3 (Optima-preserving sparse embedding). A sparse embedding matrix is *optima-preserving* if each target dimension (i.e., each column in S) contains at most one active input dimension.

Definition 4 (Sparse function / function with an active subspace). Let $\mathcal{X} = [-1, 1]^D$. A function $f : \mathcal{X} \rightarrow \mathbb{R}$ has an *active subspace* (or *effective subspace* [71]), if there exist a subspace (i.e., a space $\mathcal{Z} \subseteq \mathbb{R}^{d_e}$, with $d_e \leq D$ where $d_e \in \mathbb{N}_{++}$ is the effective dimensionality and $\mathbb{N}_{++} = \mathbb{N} \setminus \{0\}$) and a projection matrix $S^\top \in \mathbb{R}^{D \times d_e}$, such that for any $\mathbf{x} \in \mathcal{X}$ there exists a $\mathbf{z} \in \mathcal{Z}$ so that $f(\mathbf{x}) = f(S^\top \mathbf{z})$ and d_e is the smallest integer with this property. The function is called *sparse* if it has an active subspace and S^\top is a sparse embedding matrix and $\mathcal{Z} = [-1, 1]^{d_e}$.

A.1 Proof of Theorem 1

We prove the worst-case success probability for the BAXUS embedding.

Theorem 1 (Worst-case success probability of the BAXUS embedding). Let D be the input dimensionality and $d \geq d_e$ the dimensionality of the embedding. Let $\beta_{\text{small}} = \lfloor \frac{D}{d} \rfloor$ and $\beta_{\text{large}} = \lceil \frac{D}{d} \rceil$ be the small and large bin sizes. Then the probability of Y^* (see Definition 2) for the BAXUS embedding is

$$p_B(Y^*; D, d, d_e) = \frac{\sum_{i=0}^{d_e} \binom{d(1+\beta_{\text{small}})-D}{i} \binom{D-d\beta_{\text{small}}}{d_e-i} \beta_{\text{small}}^i \beta_{\text{large}}^{d_e-i}}{\binom{D}{d_e}}. \quad (4)$$

Proof. The assignment of input dimensions to target dimensions and the signs of the input dimensions fully define the BAXUS embedding. Note that the signs do not affect $p_B(Y^*; D, d, d_e)$ because they only correspond to “flipping” the input dimension in the target space, and our construction ensures that the value ranges are symmetric to the origin.

An assignment is optima-preserving if and only if it is possible to find a point in \mathcal{Y} that maps to an optimum in \mathcal{X} for any f . The “only if” is true because f is assumed to be sparse with an active subspace with d_e active dimensions. This means that the optima in \mathcal{X} only change their function values along the d_e active dimensions. Suppose it is possible to find a point in \mathcal{Y} that maps to an arbitrary optimum in \mathcal{X} . In that case, the assignment is optima-preserving because it can individually adjust all the d_e active dimensions in \mathcal{X} . However, this generally requires each active input dimension to be mapped to a distinct target dimension (note that we require being able to represent the optimum for *any* f). Otherwise, there would be at least two active input dimensions that cannot be changed independently. Therefore, the probability of Y^* equals the probability of an optima-preserving assignment.

As all assignments are equally likely under the construction, the probability of an assignment being optima-preserving is equal to the number of possible optima-preserving assignments divided by the total number of assignments. There are $\binom{D}{d_e}$ ways of distributing the d_e active dimensions across the D positions, giving the denominator in Eq. (4).

Let us first assume that $\beta_{\text{small}} = \beta_{\text{large}} = \beta$, i.e., all target dimensions have the same number of input dimensions and d divides D . We refer to this case as the *balanced case*. There are $\binom{d}{d_e}$ ways of distributing the d_e active dimensions across the d different target dimensions. Given one active dimension, there are β ways in which this dimension can map to the target dimension. Therefore, for the balanced case, the worst-case success probability is given by

$$p_B(Y^*; D, d, d_e) = \frac{\beta^{d_e} \binom{d}{d_e}}{\binom{D}{d_e}}. \quad (5)$$

Next, we generalize Eq. (5) for cases where d does not divide D . We refer to this case as the *near-balanced case*. In that case, there are two bin sizes: β_{small} and β_{large} with $\beta_{\text{large}} = \beta_{\text{small}} + 1$. There are $d\beta_{\text{large}} - D$ small bins (i.e., bins with bin size β_{small}) and $D - d\beta_{\text{small}}$ large bins: $D - d\beta_{\text{small}}$ gives the number of input dimensions that would not be covered if all bins were small. Since β_{small} and β_{large} differ by 1, this also gives the number of bins that have to be large. Conversely, if we only had large bins, we would cover $d\beta_{\text{large}} - D$ too many input dimensions. Therefore, we need $D - d\beta_{\text{small}}$ large and $d\beta_{\text{large}} - D$ small bins.

We consider all ways of distributing the d_e active dimensions across the $d\beta_{\text{large}} - D$ small and $D - d\beta_{\text{small}}$ large bins so that there is at most one active dimension in each bin. Recall that this number gives the numerator in Eq. (4). For a conflict-free assignment, if i active dimensions are mapped to small bins, then $d_e - i$ active dimensions must be assigned to large bins. There are $\binom{d(1+\beta_{\text{small}})-D}{i} \binom{D-d\beta_{\text{small}}}{d_e-i}$ such assignments. Here we use that $1 + \beta_{\text{small}} = \beta_{\text{large}}$ holds for the near-balanced case. Recall that each small bin has β_{small} locations and that each large bin has β_{large} locations that an active dimension can be assigned to. Because $0 \leq i \leq d_e$ by construction, the number of assignments that result in an optima-preserving embedding is

$$\sum_{i=0}^{d_e} \binom{d(1+\beta_{\text{small}})-D}{i} \binom{D-d\beta_{\text{small}}}{d_e-i} \beta_{\text{small}}^i \beta_{\text{large}}^{d_e-i}.$$

Note that we leverage the facts $\binom{0}{0} = 1$, $\binom{0}{x} = 0$ for all $x \geq 1$, $\binom{y}{x} = 0$ if $x > y \geq 0$, and $\binom{x}{0} = 1$ for all x , thus the sum is well defined. Recall that we already showed that the denominator is $\binom{D}{d_e}$. Therefore, Eq. (4) gives the success probability in the near-balanced case.

It is easy to see that Eq. (4) is equivalent to the near-balanced formulation in Eq. (5) when d divides D . When d divides D , $\beta_{\text{small}} = \beta_{\text{large}} = \beta$, $d(1 + \beta_{\text{small}}) - D = d$, and $D - d\beta_{\text{small}} = 0$. Therefore, the worst-case success probability for the near-balanced case is given by

$$\begin{aligned} p_B(Y^*; D, d, d_e) &= \frac{\sum_{i=0}^{d_e} \binom{d(1+\beta_{\text{small}})-D}{i} \binom{D-d\beta_{\text{small}}}{d_e-i} \beta_{\text{small}}^i \beta_{\text{large}}^{d_e-i}}{\binom{D}{d_e}} \\ &\stackrel{\beta_{\text{small}}=\beta_{\text{large}}}{=} \frac{\sum_{i=0}^{d_e} \binom{d}{i} \binom{0}{d_e-i} \beta^i \beta^{d_e-i}}{\binom{D}{d_e}} \\ &= \frac{\beta^{d_e} \sum_{i=0}^{d_e} \binom{d}{i} \binom{0}{d_e-i}}{\binom{D}{d_e}} = \frac{\beta^{d_e} \binom{d}{d_e}}{\binom{D}{d_e}} \end{aligned}$$

where the last equality is true because the sum is zero unless $i = d_e$. □

A.2 Proof of Corollary 2

We prove the optimality of the BAXUS embedding in terms of the worst-case success probability.

Corollary 2. With the same input, target, and effective dimensionalities (D , d , and d_e), no sparse embedding has a higher worst-case success probability than the BAXUS embedding.

Proof. By Definition 1, an embedding matrix $S \in \{0, \pm 1\}^{D \times d}$ is sparse if each row in S has exactly one non-zero entry. Such an embedding can always be interpreted as disjoint sets of signed input dimensions assigned to different target dimensions: For the n -th input dimension, find the column with the non-zero. The respective column gives the target dimension; the entry in the matrix itself gives the sign. Conversely, each target dimension has a set of contributing input dimensions, and we call the set of input dimensions mapping to a target dimension a “bin”. The sign of the input dimensions does not influence the success probability as it does not influence the ability of an embedding to contain the optimum.

We will prove that the BAXUS embedding is optimal, i.e., every other sparse embedding has a worst-case success probability that is lower or equal. We start by giving the worst-case success probability for arbitrary bin sizes.

Let β_n be the bin size of the n -th bin. By Definition 2, a success is guaranteed if each bin contains at most one active input dimension. Therefore, the worst-case success probability for arbitrary bin sizes has to consider the number of cases where each bin contains at most one active input dimension and the number of bins containing one active input dimension is equal to the number of active input dimensions d_e . In a bin of size β_i , the active input dimension can lie in β_i different locations. Bins not containing an active dimension do not contribute to the worst-case success probability.

We suppose w.l.o.g. that $D \geq d$. Thus, every target dimension has at least one input dimension. For each n from 1 to d , let the value i_n indicate whether the n -th bin (or target dimension) contains an active dimension ($i_n = 1$) or not ($i_n = 0$). The indicator variable $\mathbb{1}_{(\sum_{n=1}^d i_n)=d_e}$ ensures that only cases where exactly d_e bins contain an active input dimension are counted. Note that $\sum_{i_1=0}^1 \sum_{i_2=0}^1 \cdots \sum_{i_d=0}^1 \mathbb{1}_{(\sum_{n=1}^d i_n)=d_e} = \binom{d}{d_e}$. For each case where the d_e active dimensions are assigned to d_e out of d disjoint bins, the term $\prod_{n=1}^d \beta_n^{i_n}$ accounts for the locations in which the active dimension can lie in the n -th bin. Other cases do not contribute to the worst-case success probability. The exponent ensures that only bins containing an active dimension contribute to the denominator.

Then the worst-case success probability for arbitrary bin sizes is given by

$$p_{\text{general}}(Y^*; D, d, d_e) = \frac{\overbrace{\sum_{i_1=0}^1 \sum_{i_2=0}^1 \cdots \sum_{i_d=0}^1 \mathbb{1}_{(\sum_{n=1}^d i_n)=d_e} \prod_{n=1}^d \beta_n^{i_n}}^{=\binom{d}{d_e}}}{\binom{D}{d_e}}, \quad (6)$$

with $\beta_n > 0$, $\sum_{n=1}^d \beta_n = D$, and $d \geq d_e$:

As in Theorem 1, the denominator of Eq. (6) gives all ways of assigning d_e active dimensions to D input dimensions.

We now prove that any sparse embedding has a worst-case success probability that is less or equal to the worst-case success probability of the BAXUS embedding.

Let β_{small} , β_{large} , and $p_B(Y^*; D, d, d_e)$ as in Theorem 1. Then,

$$p_{\text{general}}(Y^*; D, d, d_e) \leq p_B(Y^*; D, d, d_e) = \frac{\overbrace{\sum_{i=0}^{d_e} \binom{d(1+\beta_{\text{small}})-D}{i} \binom{D-d\beta_{\text{small}}}{d_e-i} \beta_{\text{small}}^i \beta_{\text{large}}^{d_e-i}}^{=\binom{d}{d_e}}}{\binom{D}{d_e}}.$$

We refer the reader to the proof of Theorem 1 for an explanation of the binomial coefficients. The fact that $\sum_{i=0}^{d_e} \binom{d(1+\beta_{\text{small}})-D}{i} \binom{D-d\beta_{\text{small}}}{d_e-i} = \binom{d}{d_e}$ can be seen by noting that $(d(1+\beta_{\text{small}})-D) + (D-d\beta_{\text{small}}) = d$ and applying Vandermonde's convolution [25].

We will now prove that if d divides D , then the product in the numerator of Eq. (6) is maximized if all the factors are the same, i.e., $\beta = \frac{D}{d}$. We will then show that if d does not divide D , the integer-solution of maximal value is attained for $\beta_{\text{large}} - \beta_{\text{small}} = 1$.

First case (d divides D) We now show that the following holds for the term $\prod_{n=1}^d \beta_n^{i_n}$ in the numerator of Eq. (6): $\prod_{n=1}^d \beta_n^{i_n} \leq \beta^{d_e}$. The numerator in Eq. (6) can also be written as $e_{d_e}(\beta_1, \dots, \beta_d)$ where

$$\begin{aligned} e_{d_e}(\beta_1, \dots, \beta_d) &= \sum_{i_1 < i_2 < \dots < i_{d_e}} \beta_{i_1} \beta_{i_2} \cdots \beta_{i_{d_e}} \\ &= \sum_{i_1=0}^1 \sum_{i_2=0}^1 \cdots \sum_{i_d=0}^1 \mathbb{1}_{(\sum_{n=1}^d i_n)=d_e} \prod_{n=1}^d \beta_n^{i_n} \end{aligned}$$

is the d_e -th elementary symmetric function of β_1, \dots, β_d [3]. Maclaurin's inequality [3] states that

$$\frac{e_1(\beta_1, \dots, \beta_d)}{\binom{d}{1}} \geq \sqrt{\frac{e_2(\beta_1, \dots, \beta_d)}{\binom{d}{2}}} \geq \dots \geq \sqrt[d_e]{\frac{e_{d_e}(\beta_1, \dots, \beta_d)}{\binom{d}{d_e}}} \geq \dots \geq \sqrt[d]{\frac{e_d(\beta_1, \dots, \beta_d)}{\binom{d}{d}}} \quad (7)$$

In particular,

$$\frac{e_1(\beta_1, \dots, \beta_d)}{\binom{d}{1}} = \frac{\sum_{i=1}^d \beta_i}{d} = \frac{D}{d} = \beta \quad (8)$$

holds. Taking Eq. (7) and Eq. (8) to the power d_e and multiplying by $\binom{d}{d_e}$, we obtain

$$\beta^{d_e} \binom{d}{d_e} \geq e_{d_e}(\beta_1, \dots, \beta_d) = \sum_{i_1=0}^1 \sum_{i_2=0}^1 \dots \sum_{i_d=0}^1 \mathbb{1}_{(\sum_{n=1}^d i_n)=d_e} \prod_{n=1}^d \beta_n^{i_n}, \quad (9)$$

with equality if and only if $\beta_i = \beta_j$ for $i, j \in \{1, \dots, n\}$ [3]. Therefore, the product in the numerator of Eq. (6) is maximized if all factors are equal.

Second case (d does not divide D) However, if d does not divide D , then β is no integer which is not feasible in our setting. The d_e -th elementary symmetric function $e_{d_e}(\beta)$ (see Eq. (9)) is known to be *Schur-concave* if $\beta_i \geq 0$ holds for all i [44]. This condition is met by β . We use the following definition of [44]: A function $f: \mathbb{R}^d \rightarrow \mathbb{R}$ is called Schur-concave if $\gamma \prec \beta$ implies $f(\gamma) \geq f(\beta)$. Here, $\gamma \prec \beta$ means that β majorizes γ , i.e.,

$$\sum_{i=1}^k \gamma_i^\downarrow \leq \sum_{i=1}^k \beta_i^\downarrow \quad \text{for all } k \in \{1, \dots, d\}, \quad \text{and} \quad \sum_{i=1}^d \gamma_i = \sum_{i=1}^d \beta_i,$$

where γ^\downarrow and β^\downarrow are the vectors of all elements in γ and β in descending order [44].

We now show that there is no integer solution γ such that there is a near-balanced solution that majorizes γ .

For some near-balanced assignment β of small and large bins to the d target dimensions, consider the vector

$$\beta^\downarrow = \left(\underbrace{\left(\overset{=\beta_{\text{large}}}{\left\lfloor \frac{D}{d} \right\rfloor}, \dots, \left\lfloor \frac{D}{d} \right\rfloor \right)}_{D - d\beta_{\text{small}} \text{ many}}, \underbrace{\left(\overset{=\beta_{\text{small}}}{\left\lfloor \frac{D}{d} \right\rfloor}, \dots, \left\lfloor \frac{D}{d} \right\rfloor \right)}_{d\beta_{\text{large}} - D \text{ many}} \right)$$

of bin sizes in decreasing order. For any other BAXUS embedding given by some permutation β' of β , it holds that $\beta'^\downarrow = \beta^\downarrow$. Note that for any assignment $\gamma = \{\gamma_1, \dots, \gamma_d\}$ of bin sizes over the d target dimensions, it has to hold that

$$\sum_{i=1}^d \gamma_i = D; \quad \gamma_i \geq 0, \quad i \in \{1, \dots, d\}; \quad \gamma \in \mathbb{N}_0^d.$$

By assumption, since we are in the near-balanced case, $\beta_{\text{small}} = \beta_{\text{large}} - 1$.

Assume there exists an assignment of bin sizes γ that is not a permutation of β such that $\gamma \prec \beta$, i.e.,

$$\sum_{i=1}^k \gamma_i^\downarrow \leq \sum_{i=1}^k \beta_i^\downarrow \quad \text{for all } k \in \{1, \dots, d\},$$

and

$$\sum_{i=1}^d \gamma_i = \sum_{i=1}^d \beta_i,$$

and

$$\exists j : \gamma_j^\downarrow < \beta_j^\downarrow.$$

Let κ denote the (non-empty) set of such indices. Because the elements of β and γ both sum up to D , it has to hold for all $\kappa \in \kappa$ that

$$\sum_{i=1, i \neq \kappa}^d \gamma_i^\downarrow > \sum_{i=1, i \neq \kappa}^d \beta_i^\downarrow. \quad (10)$$

Remember that β only contains elements of sizes β_{small} and β_{large} with $\beta_{\text{large}} = \beta_{\text{small}} - 1$. Then, Eq. (10) can only hold if either 1) γ contains more elements of size β_{large} than β or 2) if it contains at least one element that is larger than β_{large} , the largest element in β .

Both cases lead to a contradiction. In the first case,

$$\sum_{i=1}^{D-d\beta_{\text{small}}+1} \gamma_i^\downarrow > \sum_{i=1}^{D-d\beta_{\text{small}}+1} \beta_i^\downarrow \Rightarrow \gamma \not\leq \beta$$

since at least the first $D - d\beta_{\text{small}} + 1$ elements of γ^\downarrow are $\lceil \frac{D}{d} \rceil$ but only the first $D - d\beta_{\text{small}}$ elements of β^\downarrow are $\lceil \frac{D}{d} \rceil$ and the $D - d\beta_{\text{small}} + 1$ -th element of β^\downarrow is $\lceil \frac{D}{d} \rceil - 1$.

In the second case, $\gamma \not\leq \beta$ because $\gamma_1^\downarrow > \beta_1^\downarrow$. It follows that no such γ exists. Therefore, the BAXUS embedding has a maximum worst-case success probability among sparse embeddings. \square

A.3 Proof of Corollary 1

Corollary 1. For $D \rightarrow \infty$, the worst-case success probability of the BAXUS embedding is

$$\lim_{D \rightarrow \infty} p_B(Y^*; D, d, d_e) = \frac{d!}{(d - d_e)!d^{d_e}},$$

and hence matches HESBO's worst-case success probability $p_H(Y^*; d, d_e)$.

Proof. By Corollary 1, the following holds for arbitrary $1 \leq d_e \leq d \leq D$ where $d, d_e, D \in \mathbb{N}_{++}$:

$$\frac{d!}{(d - d_e)!d^{d_e}} \leq p_B(Y^*; D, d, d_e),$$

because $\frac{d!}{(d - d_e)!d^{d_e}}$ is HESBO's worst-case success probability and hence less or equal to the worst-case success probability of BAXUS.

Furthermore, by the proof of Corollary 1,

$$p_B(Y^*; D, d, d_e) \leq \frac{\beta^{d_e} \binom{d}{d_e}}{\binom{D}{d_e}},$$

because $\frac{\beta^{d_e} \binom{d}{d_e}}{\binom{D}{d_e}}$ is larger or equal the worst-case success probability of any sparse embedding, among

which BAXUS is the embedding with maximum worst-case success probability and $\frac{\beta^{d_e} \binom{d}{d_e}}{\binom{D}{d_e}} = p_B(Y^*; D, d, d_e)$ if and only if $\beta_{\text{small}} = \beta_{\text{large}}$, i.e., d divides D .

In summary, we have

$$\frac{d!}{(d - d_e)!d^{d_e}} \leq p_B(Y^*; D, d, d_e) \leq \frac{\beta^{d_e} \binom{d}{d_e}}{\binom{D}{d_e}}.$$

We now show that, for fixed d and d_e , the sequences $\frac{d!}{(d - d_e)!d^{d_e}}$ and $\frac{\beta^{d_e} \binom{d}{d_e}}{\binom{D}{d_e}}$ converge to the same point as $D \rightarrow \infty$. We consider $\lim_{\beta \rightarrow \infty}$, which is equivalent to $\lim_{D \rightarrow \infty}$ as $\beta = \frac{D}{d}$ and d is fixed. Note, that we can consider $\beta = \frac{D}{d}$ even though it is not a valid success probability when d does not

divide D , since we are only interested in bounding the true success probability. Then,

$$\begin{aligned} \lim_{\beta \rightarrow \infty} \frac{\beta^{d_e} \binom{D}{d_e}}{\binom{D}{d_e}} &= \lim_{\beta \rightarrow \infty} \frac{\beta^{d_e} d! (D - d_e)!}{D! (d - d_e)!} \\ &= \lim_{\beta \rightarrow \infty} \frac{\beta^{d_e} d! (\beta d - d_e)!}{(\beta d)! (d - d_e)!} \\ &= \lim_{\beta \rightarrow \infty} \beta^{d_e} \frac{d!}{(d - d_e)!} \frac{(\beta d - d_e)!}{(\beta d)!} \end{aligned}$$

Applying Stirling's approximation [25] to the numerator and the denominator of the last factor, we obtain

$$\begin{aligned} &= \lim_{\beta \rightarrow \infty} \beta^{d_e} \frac{d!}{(d - d_e)!} \frac{\sqrt{2\pi(\beta d - d_e)} \left(\frac{\beta d - d_e}{e}\right)^{\beta d - d_e} r(\beta d - d_e)}{\sqrt{2\pi\beta d} \left(\frac{\beta d}{e}\right)^{\beta d} r(\beta d)} \\ &= \lim_{\beta \rightarrow \infty} \beta^{d_e} \frac{d!}{(d - d_e)!} \sqrt{\frac{\beta d - d_e}{\beta d}} e^{d_e} \frac{(\beta d - d_e)^{\beta d - d_e} r(\beta d - d_e)}{(\beta d)^{\beta d} r(\beta d)} \\ &= \lim_{\beta \rightarrow \infty} \beta^{d_e} \frac{d!}{(d - d_e)!} \sqrt{\frac{\beta d - d_e}{\beta d}} e^{d_e} \left(\frac{\beta d - d_e}{\beta d}\right)^{\beta d} \frac{1}{(\beta d - d_e)^{d_e}} \frac{r(\beta d - d_e)}{r(\beta d)} \\ &= \lim_{\beta \rightarrow \infty} \frac{d!}{(d - d_e)!} \sqrt{\frac{\beta d - d_e}{\beta d}} e^{d_e} \left(\frac{\beta d - d_e}{\beta d}\right)^{\beta d} \frac{\beta^{d_e}}{(\beta d - d_e)^{d_e}} \frac{r(\beta d - d_e)}{r(\beta d)} \\ &= \lim_{\beta \rightarrow \infty} \frac{d!}{(d - d_e)!} \underbrace{\sqrt{\frac{\beta d - d_e}{\beta d}}}_{\rightarrow 1} e^{d_e} \underbrace{\left(\frac{\beta d - d_e}{\beta d}\right)^{\beta d}}_{\rightarrow e^{-d_e}} \underbrace{\left(\frac{1}{d}\right)^{d_e}}_{= d^{-d_e}} \underbrace{\left(\frac{\beta d}{\beta d - d_e}\right)^{d_e}}_{\rightarrow 1} \underbrace{\frac{r(\beta d - d_e)}{r(\beta d)}}_{\rightarrow 1} \\ &= \frac{d!}{(d - d_e)! d^{d_e}} \end{aligned}$$

where the following holds for the error term $r(x)$ of the Stirling approximation [56]:

$$\exp\left(\frac{1}{12x+1}\right) \leq r(x) \leq \exp\left(\frac{1}{12x}\right).$$

Then, $\frac{r(\beta d - d_e)}{r(\beta d)} \rightarrow 1$ for $\beta \rightarrow \infty$ holds since

$$\begin{aligned} \frac{r(\beta d - d_e)}{r(\beta d)} &\leq \exp\left(\frac{1}{12(\beta d - d_e)} - \frac{1}{12\beta d + 1}\right) \\ &= \exp\left(\frac{12d_e + 1}{12^2\beta^2 d^2 + 12\beta d - 12^2\beta d d_e - 12d_e}\right) \\ &= \exp\left(\frac{d_e + \frac{1}{12}}{\beta d(12\beta d + 1 - 12d_e) - d_e}\right), \end{aligned}$$

and

$$\begin{aligned} \frac{r(\beta d - d_e)}{r(\beta d)} &\geq \exp\left(\frac{1}{12(\beta d - d_e) + 1} - \frac{1}{12\beta d}\right) \\ &= \exp\left(\frac{12d_e - 1}{12^2\beta^2 d^2 + 12\beta d - 12^2\beta d d_e - 12\beta d_e}\right) \\ &= \exp\left(\frac{d_e - \frac{1}{12}}{\beta d(12\beta d + 1 - 12d_e) - d_e}\right), \end{aligned}$$

which both go to 1 as $\beta \rightarrow \infty$.

Hence, BAXUS' worst-case success probability is bounded from below and above by sequences that converge to the same point as $D \rightarrow \infty$. The squeeze theorem (e.g., [62]) implies

$$\lim_{D \rightarrow \infty} p_B(Y^*; D, d, d_e) = \frac{d!}{(d - d_e)! d^{d_e}}.$$

□

B Consistency of BAXUS

We prove the global convergence of function values for BAXUS. The proof idea is similar to Eriksson and Poloczek [21] but relaxes the assumption of a unique global minimizer. By construction, f is sparse (see Definition 4), i.e., there exists a set of dimensions of f that do not influence the function value. Thus, an optimal solution stays optimal regardless of how inactive dimensions are set. This is why we must relax the assumption of a unique global minimizer in the input space. Instead, we assume a unique global minimizer in the active subspace $\mathbf{z}^* \in \mathcal{Z}$ that can map to arbitrarily many minimizers in the input space. Note that this assumption covers the case when the target space corresponds to the input space, i.e., $d = D$.

Theorem 2 (BAXUS consistency). *With the following definitions:*

- D1. $\{\mathbf{x}_k\}_{k=1}^\infty$ is a sequence of points of decreasing function value;
- D2. $\mathbf{x}^* \in \arg \min_{\mathbf{x} \in \mathcal{X}} f(\mathbf{x})$ is a minimizer in \mathcal{X} ;

and under the following assumptions:

- A1. D is finite;
- A2. f is observed without noise;
- A3. f is sparse and bounded in \mathcal{X} , i.e., $\exists C \in \mathbb{R}_{++}$ s.t. $|f(\mathbf{x})| < C \forall \mathbf{x} \in \mathcal{X}$;
- A4. At least one of the minimizers \mathbf{x}_i^* lies in a continuous region with positive measure;
- A5. Once BAXUS reached the input dimensionality D , the initial points $\{\mathbf{x}_i\}_{i=1}^{n_{\text{init}}}$ after each TR restart for BAXUS are chosen such that $\forall \delta \in \mathbb{R}_{++}$ and $\mathbf{x} \in \mathcal{X}$, $\exists \nu(\mathbf{x}, \delta) > 0$: $\mathbb{P}(\exists i : \|\mathbf{x} - \mathbf{x}_i\|_2 \leq \delta) \geq \nu(\mathbf{x}, \delta)$, i.e., the probability that at least one point in $\{\mathbf{x}_i\}_{i=1}^{n_{\text{init}}}$ ends up in a ball centered at \mathbf{x} with radius δ is at least $\nu(\mathbf{x}, \delta)$;

$f(\mathbf{x}_k)$ converges to $f(\mathbf{x}^*)$ with probability 1.

Proof. We first show that BAXUS must eventually arrive at an embedding equivalent to the input space. By Assumption A1, the number of accepted “failures” (i.e., the number of times BAXUS needs to fail in finding a better solution until the TR base length is shrunk) is always finite since it is always bounded by the target dimension ($\forall i \tau_{\text{fail}}^i \leq d_i$) which is at most equal to D ($\forall i d_i \leq D$). By the facts that BAXUS considers any sampled point an improvement only if it improves over the current best solution by at least some constant $\gamma \in \mathbb{R}_{++}$ and that f is bounded (Assumption A3), BAXUS can only perform a finite number of function evaluations without increasing the target dimensionality of its embedding.

Once BAXUS reaches D , it behaves like TURBO [22] for which Eriksson and Poloczek [21] proved global convergence assuming a unique global minimizer. For the case $d_e < D$, we notice that multiple minima in the input space occur due to inactive dimensions that do not influence the function value.

The remainder of our proof is based on the convergence theorem for global search by Solis and Wets [63], which proves convergence of function values for random search with possibly multiple minima. By considering the sequence

$$\left\{ \mathbf{x}'_i \in \arg \min_{\hat{\mathbf{x}} \in \{\mathbf{x}_k\}_{k=1}^i} f(\hat{\mathbf{x}}) \right\}_{i=1}^\infty$$

of points of decreasing function values where $\{\mathbf{x}_k\}_{k=1}^i$ are the observations up to the i -th function evaluation, Definition D1 is satisfied. Additionally, by the fact that, at each TR restart, BAXUS performs random restarts with uniform probability on \mathcal{X} , BAXUS satisfies the assumptions of the theorem by Solis and Wets [63].

The theorem by Solis and Wets [63] states that for a sequence $\{\mathbf{x}_k\}_{k=1}^\infty$ of sampling points with $\varepsilon \in \mathbb{R}_{++}$,

$$\begin{aligned} \lim_{k \rightarrow \infty} \mathbb{P}[\mathbf{x}_k \in R_\varepsilon] &= 1 \\ R_\varepsilon &= \{\mathbf{x} \in \mathcal{X} : f(\mathbf{x}) < \alpha + \varepsilon\} \\ \alpha &= \inf\{t : v(\mathbf{x} \in \mathcal{X} : f(\mathbf{x}) < t) > 0\} \end{aligned}$$

where R_ε is the set of ε -optimal function values, α is the *essential infimum*, and v is the Lebesgue measure. Note that the essential infimum α is equal to the minimum if the minimizer lies in a continuous region of positive measure, i.e., $\alpha = f(\mathbf{x}_i^*)$. By Assumption A4 and by letting $\varepsilon \rightarrow 0$, $f(\mathbf{x}_k)$ converges to $f(\mathbf{x}_i^*)$. \square

C Additional empirical evaluations

C.1 Ablation study for the BAXUS embedding

We conduct an ablation study to investigate the difference between the BAXUS and HESBO embeddings. We run TURBO of Eriksson et al. [22] in an embedded subspace with the two different embeddings. We use a version of ACKLEY10 (ten active dimensions, i.e., $d_e = 10$), where we shift the optimum away from the origin with a uniformly random vector $\boldsymbol{\delta} \in [-32.768, 32.768]^{d_e}$ with $\delta_i \sim \mathcal{U}(-32.768, 32.768)$. The function we optimize is then

$$f_{\text{ShiftedAckley10}}(\mathbf{x}) = f_{\text{Ackley10}}(\mathbf{x} + \boldsymbol{\delta}).$$

We adjust the boundaries of the search space such that $f_{\text{ShiftedAckley10}}$ is evaluated on the domain $\mathcal{X} = [-32.768, 32.768]^{d_e}$. The reason for shifting the optimum is that the original ACKLEY function has its optimum at the origin. In that case, any sparse embedding contains this optimum, even if all the active input dimensions are mapped to the same target dimension.

We add 10 dummy dimensions, such that $D = 30$ and set $d = 20$. With this problem-setting, the BAXUS and HESBO embeddings have a probability of approximately 0.27 and 0.07 of containing the optimum, respectively.

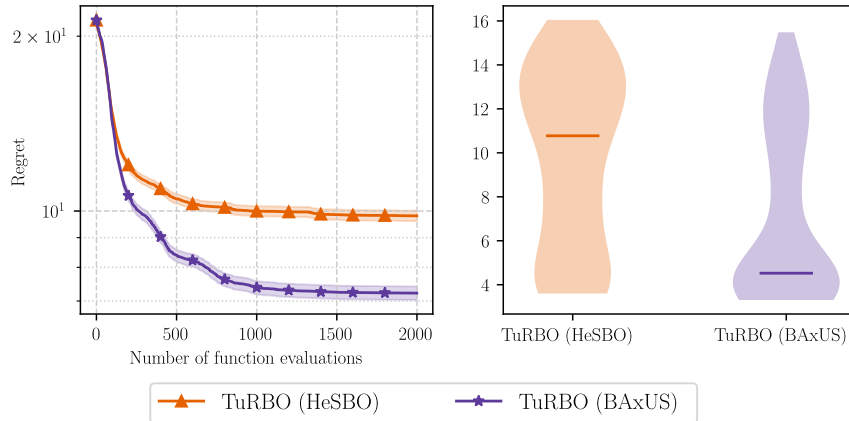


Figure 5: **Left:** the BAXUS embedding gives better optimization performance on the shifted ACKLEY10 function: TURBO in embedded subspaces of the BAXUS and HESBO embeddings. The BAXUS embedding has a higher probability to contain the optimum. **Right:** the distribution of the final incumbents (lower the better). The horizontal bars show the median.

The left side of Figure 5 shows the incumbent mean for TURBO in the two different embedded subspaces. The shaded regions show one standard error. TURBO in an BAXUS embedding has

significantly better optimization performance than in a HESBO embedding. The right side of Figure 5 shows the distributions of the final incumbents and their median. The BAXUS embedding leads to a significantly lower median and only rarely a similarly bad embedding as the HESBO method when combined with TURBO.

We perform a two-sided Wilcoxon rank-sum statistical test to check the difference between the best observed function values for the two embeddings. The difference is significant with $p \approx 0.00001$.

The performance difference between the two embeddings depends on the characteristics of the function and the different dimensionalities, the input dimensionality D , the target dimensionality d , and the effective dimensionality d_e . For problems with few active dimensions and many input dimensions, the BAXUS and HESBO embeddings become more similar (see Figure 2). However, by Corollary 2, the BAXUS embedding is, in expectation and in terms of the worst-case success probability, better than the HESBO embedding for arbitrary sparse functions.

For functions with an optimum at the origin, both embeddings contain that optimum regardless of d : Even if all active input dimensions are mapped to the same target dimension, the optimum in the input space can be reached by “setting” this particular target dimension to zero.

TURBO with BAXUS embedding vs. BAXUS. We compare the simple idea of running TURBO in a BAXUS embedding of fixed target dimensionality with the BAXUS algorithm described in Section 3. We run this simple approach for 11 different target dimensionalities d (2, 10, 20, . . . , 100) on the LASSO-HARD benchmark and show the results with a sequential color map in Figure 6. Only the first $d = 2$ -dimensional embedding achieves the same initial speedup as BAXUS, which is expected as BAXUS starts in a similarly low-dimensional initial embedding. However, the fixed embedding cannot explore the input space sufficiently and has the worst final solution. High-dimensional fixed embeddings have more freedom in exploring the input space; however, they suffer from slower initial optimization performance.

BAXUS has the same initial speedup as the two-dimensional fixed embedding but can explore the space further by increasing the dimensionality of its embedding.

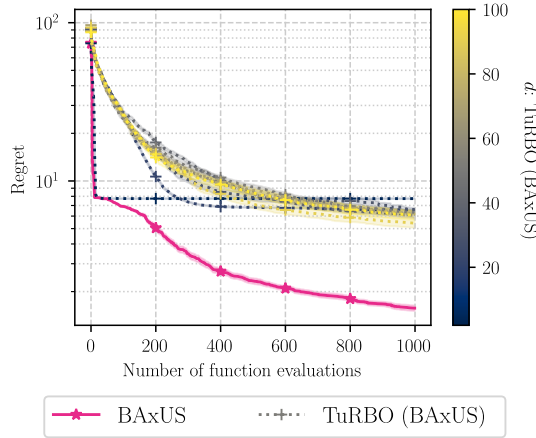


Figure 6: An evaluation of BAXUS and TURBO with BAXUS embeddings of different target dimensionalities on LASSO-HARD: We run TURBO with the BAXUS embedding for fixed target dimensionalities $d = 2, 10, 20, \dots, 100$ and compare to BAXUS.

Summing up, we observe that BAXUS achieves a better performance than TURBO with a fixed embedding dimensionality.

C.2 Evaluation on an additional Lasso benchmark

In addition to the synthetic LASSO-HIGH and LASSO-HARD benchmarks studied in Section 4, we evaluate BAXUS on the LASSO-DNA benchmark from LASSOBENCH [59]. The LASSO-DNA benchmark is a biomedical classification task, taking binarized DNA sequences as input [59].

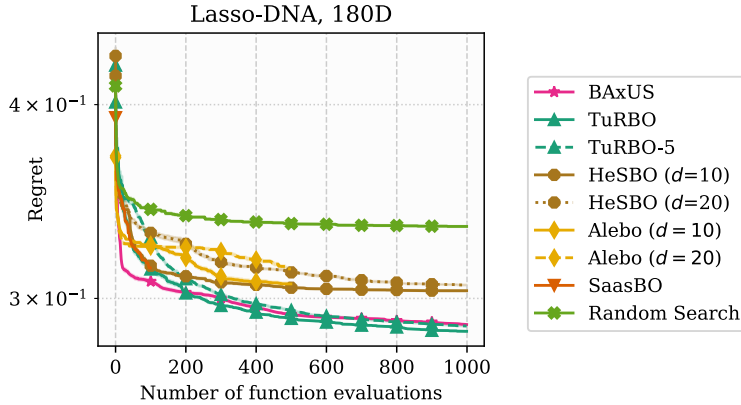


Figure 7: BAXUS and baselines on LASSO-DNA. As before, BAXUS makes considerable progress in the beginning and converges faster than TURBO and CMA-ES.

Figure 7 shows the mean performance of BAXUS on the LASSO-DNA. Each line shows the incumbent mean; the shaded regions around the lines show one standard error. We see the same qualitative behavior as discussed in Section 4: BAXUS reaches a good initial solution faster than any other method.

After a worse start, TURBO finds slightly better solutions than BAXUS.

C.3 Evaluation on additional MuJoCo benchmarks

We evaluate BAXUS with the same baselines as in Section 4. We use the implementation of [70]², in particular we use the Gym environments Ant, Swimmer, Half-Cheetah, Hopper, Walker 2D, and Humanoid 2D, all in version 2. For the 6392-dimensional Humanoid benchmark, we limit the target dimensionality of BAXUS to 1000 dimensions to keep the split budgets sufficiently large. For the other benchmarks, we do not limit the target dimensionality. Due to the high variance between runs, we ran all methods for 50 different runs.

We summarize the results in Fig. 8. We observe that BAXUS obtains equal or better solutions than the competitors on four out of six benchmarks. On the 120-dimensional Walker benchmark, BAXUS is the clear winner, followed by TURBO and CMA-ES. On the 888-dimensional Ant benchmark, HESBO finds the best solutions, followed by BAXUS that outperforms TURBO and CMA-ES. For the 102-dimensional Half-Cheetah, TURBO produces the best solutions, followed by CMA-ES and BAXUS; here, the subspace-based approaches (ALEBO and HESBO) find significantly worse solutions. For the 6392-dimensional Humanoid 2D, CMA-ES obtains the best solutions, followed by BAXUS, ALEBO, and HESBO.

D The nested family of random embeddings

We describe the method for increasing the target dimensionality under the retention of the observations. Suppose that we have collected n observations and are in target dimension d when Algorithm 2 is invoked. Algorithm 2 loops over the target dimensions $1, \dots, d$. For each target dimension, the contributing input dimensions are randomly re-assigned to new bins of given sizes. This can, for example, be realized by first randomly permuting the list of contributing input dimensions, and then dividing the list into $b + 1$ chunks (bins). If the number of contributing input dimensions is less than $b + 1$ (remember that b is the number of *new* bins), then it is not possible to re-assign the contributing input dimensions to $b + 1$ bins. Therefore, we re-assign the contributing input dimensions to $\hat{b} = \min(b, l_s - 1)$ new bins, where l_s is the number of contributing input dimensions to the s -th target dimension. This also ensures that the target dimension never grows larger than D in the BAXUS embedding. We evenly distribute the l_s contributing input dimensions across the \hat{b} bins by

²<https://github.com/facebookresearch/LA-MCTS/blob/main/example/mujoco/functions.py>, last accessed: 06/10/2022

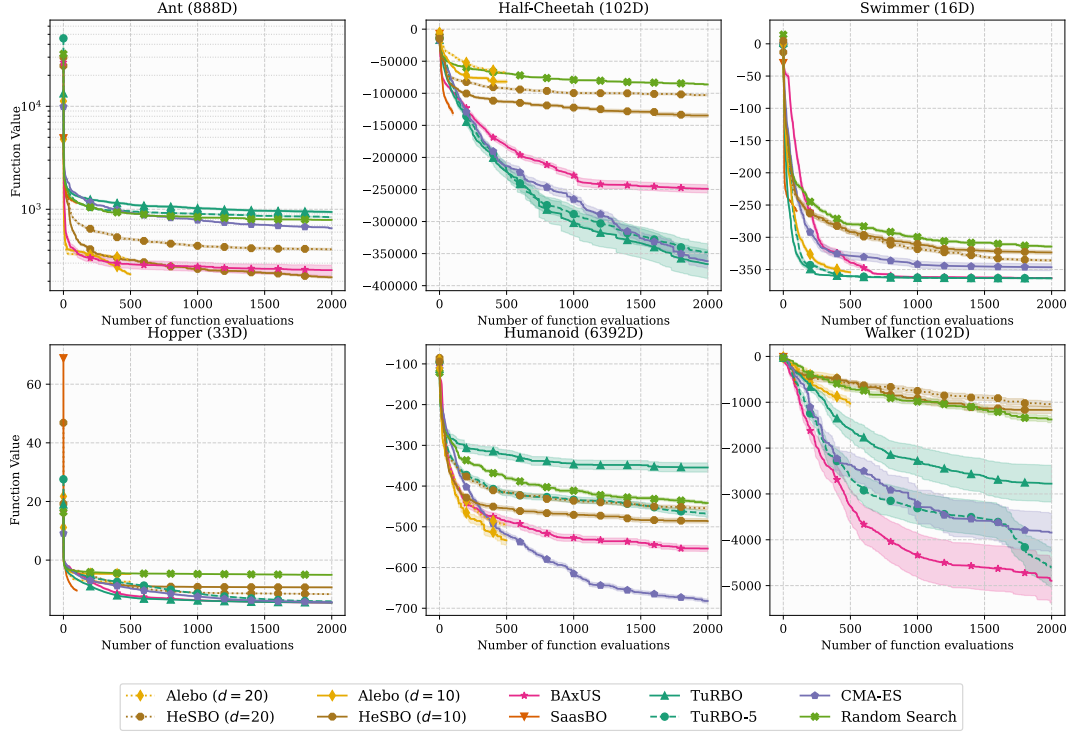


Figure 8: An evaluation of BAXUS and other methods on high-dimensional test problems of MuJoCo.

again using the BAXUS embedding. This gives a smaller (in terms of number of rows) projection matrix \tilde{S}^\top which we finally use to update S^\top :

Algorithm 2 Observation-preserving embedding increase

Input: transposed embedding matrix S^\top , number of new bins per latent dimension b , observed points $Y \in [-1, 1]^{n \times d}$.

Output: updated transposed embedding matrix S^\top and updated observation matrix Y

for $s \in \{1, \dots, d\}$ **do**

$D^s \leftarrow$ contributing input dimensions of s -th latent dimension of the current embedding

$l_s \leftarrow |D^s|$

$\hat{b} \leftarrow \min(b, l_s - 1)$ ▷ If $l_s - 1 < b$, we can at most create $l_s - 1$ new bins.

 Copy and append s -th column of Y \hat{b} times at the end of Y .

 Add \hat{b} zero columns at the end of S^\top .

$\sigma \leftarrow$ signs of dimensions $\in D^s$.

$\tilde{S}^\top \leftarrow$ Baxus-Embedding($l_s, \hat{b} + 1$) ▷ Re-assign input dims. equally³, $\tilde{S}^\top \in \{0, \pm 1\}^{l_s \times \hat{b} + 1}$

for $i \in \{1, \dots, l_s\}, j \in \{1, \dots, \hat{b} + 1\}$ **do**

if $\tilde{S}_{ij}^\top \neq 0$ **then**

if $j > 1$ **then**

$S_{i, \hat{d} - \hat{b} - 1 + j}^\top \leftarrow \sigma_i$ ▷ Move values that fall into new bins to end of S^\top .

▷ \hat{d} : columns of S^\top

$S_{i, s}^\top \leftarrow 0$ ▷ Set value in “old” column to zero.

Return S^\top and Y .

³Equally means that all $\hat{b} + 1$ bins have roughly the same number of contributing input dimensions. The number of contributing input dimensions to the different bins differ by at most 1.

E Additional details on the implementation and the empirical evaluation

We benchmark against SAASBO, TURBO, HESBO, ALEBO, and CMA-ES:

- For SAASBO, we use the implementation from [20] (<https://github.com/martinjankowiak/saasbo>, license: none, last accessed: 05/09/2022).
- For TURBO, we use the implementation from [22] (<https://github.com/uber-research/TuRBO>, license: Uber, last accessed: 05/09/2022).
- For HESBO and ALEBO, we use the implementation from [40] (<https://github.com/facebookresearch/alebo>, license: CC BY-NC 4.0, last accessed: 05/09/2022).
- For the LASSO benchmarks, we use the implementation from [59] (<https://github.com/ksehic/LassoBench>, license: MIT and BSD-3-CLause, last accessed: 05/09/2022).

We use GPyTorch (version 1.8.1) to train the GP with the following setup: We place a top-hat prior on the Gaussian likelihood noise, the signal variance, and the length scales of the Matérn 5/2 ARD kernel. The interval for the noise is $[0.005, 0.2]$, for the signal variance $[0.05, 20]$, and for the lengthscales $[0.005, 10]$.

We evaluate on the synthetic BRANIN⁴ and HARTMANN⁵ functions. Since we augment the function with dummy dimensions, we use the same domain for x_1 and x_2 , namely $[-5, 15]^D$ for BRANIN2 and $[0, 1]^D$ for HARTMANN6.

Similar to TURBO, we sample a $\min(100d_n, 5000)$ -element Sobol sequence on which we minimize the posterior sample. To maximize the marginal log-likelihood of the GP, we sample 100 initial hyperparameter configurations. The ten best samples are further optimized using the ADAM optimizer for 50 steps.

We ran the experiments for approximately 15,000 core hours on Intel Xeon Gold 6130 CPUs provided by a compute cluster.

⁴See <https://www.sfu.ca/~ssurjano/branin.html>, last accessed: 05/09/2022

⁵See <https://www.sfu.ca/~ssurjano/hart6.html>, last accessed: 05/09/2022